ISSN 0024-4902, Lithology and Mineral Resources, 2026, Vol. 61, No. 3, pp. 287–308. © Pleiades Publishing, Ltd., 2026.

The C–O Isotope Geochemistry and Chemostratigraphic Correlation of Ordovician Deposits of the Lisino-10 Borehole Section, Northwestern Russian Plate

A. V. Zaitsev[a, *], B. G. Pokrovsky[a], G. S. Iskül[b], V. L. Kosorukov[c], and E. P. Miklyaeva[a]

[a] *Geological Institute, Russian Academy of Sciences, Moscow, 119017 Russia*

[b] *Karpinsky Russian Geological Research Institute, St. Petersburg, 199106 Russia*

[c] *Faculty of Geology, Lomonosov Moscow State University, Moscow, 119992 Russia*

**e-mail: a.v.zaitsev@bk.ru*

Received August 8, 2025; revised October 25, 2025; accepted January 12, 2026

Abstract—The borehole "Lisino-10" was drilled on the Izhora Upland, approximately 90 km southwest of St. Petersburg. This study presents the first continuous carbon and oxygen isotope curves obtained from Ordovician carbonate rocks (Latorp–Rakvere regional stages) in the northwestern part of the Russian Plate. Despite relatively small deviations in $\delta^{13}C$ values (from –2.5‰ to 1.8‰), two positive carbon isotope excursions are clearly identified in the borehole section: (1) the MDICE (Middle Darriwilian Isotopic Carbon Excursion), with a peak $\delta^{13}C$ value of 1.0‰ in the Loobu Formation, and (2) the GICE (Guttenberg Isotopic Carbon Excursion) at the Sandbian–Katian boundary, with a peak $\delta^{13}C$ value of 1.8‰ at the boundary between the Vruda and Izvara formations. In addition to these positive excursions, two negative carbon isotope events are also recognized: (1) the BDNICE (Basal Dapingian Negative Isotopic Carbon Excursion), with a minimum $\delta^{13}C$ value of –2.5‰ in the lower part of the Volkhov Formation, and (2) the LSNICE (Lower Sandbian Negative Isotopic Carbon Excursion), with a minimum $\delta^{13}C$ value of –1.0‰ in the upper part of the Viivikonna Formation. These results enable carbon-isotope chemostratigraphic correlation of the Lisino-10 section with other regional sections and establish it as a reference section for the Ordovician paleobasin of the Russian Plate.

Keywords: carbon and oxygen isotope geochemistry, chemostratigraphy, Ordovician, Russian Plate, dolomite

DOI: 10.1134/S0024490226600055

INTRODUCTION

Ordovician deposits of the northwestern Russian Plate have been studied for over 200 years, being the reference object for paleontological, biostratigraphic, and lithological research.

At the turn of 20–21st centuries, isotope chemostratigraphic studies have been developed as a new tool for the correlation of regional sections with global tectonic, climatic, and biotic events.

At present, the carbon and oxygen isotope composition was studied in many sections of the Northern and Southern Baltic regions (Ainsaar et al., 2010; Bergström et al., 2015; Kaljo et al., 2007; and others). In the Russian part of the northwestern margin of the Russian Plate, isotope studies spanned only small fragments of Ordovician succession. At the moment of this study, the Middle Darriwilian MDICE positive carbon isotopic excursion in the Putilovo quarry, Volkhov and Lynna rivers (Ainsaar et al., 2020; Rasmussen et al., 2016) and a negative BDNICE excursion in the section of the Volkhov Formation of the Babino quarry (Zaitsev and Pokrovsky, 2014) were distinguished with confidence for the considered area. This situation is partly related to the absence of stratigraphically representative sections (especially, for the Upper Ordovician) in the Russian part of Baltic-Ladoga Klint area. Core of most previously drilled holes has not preserved. A direct correlation of published isotope data on the boreholes of the Baltic region with litho- and biostratigraphic units of Russian sections is usually complicated owing to the facies differences of these rocks and some regional specifics of biota.

The Lisino borehole was drilled in 2010 on the Izhora Upland, near the village of Lisino (59.424633 N, 29.572003 E), to the southwest of St. Petersburg (Fig. 1), where it recovered the Ordovician rocks around 140 m thick (Raevskaya and Iskül, 2024). The entire Ordovician section in the Lisino-10 borehole spans a stratigraphic interval from Tremadocian to the lower Katian. The studied carbonate interval of the succes-

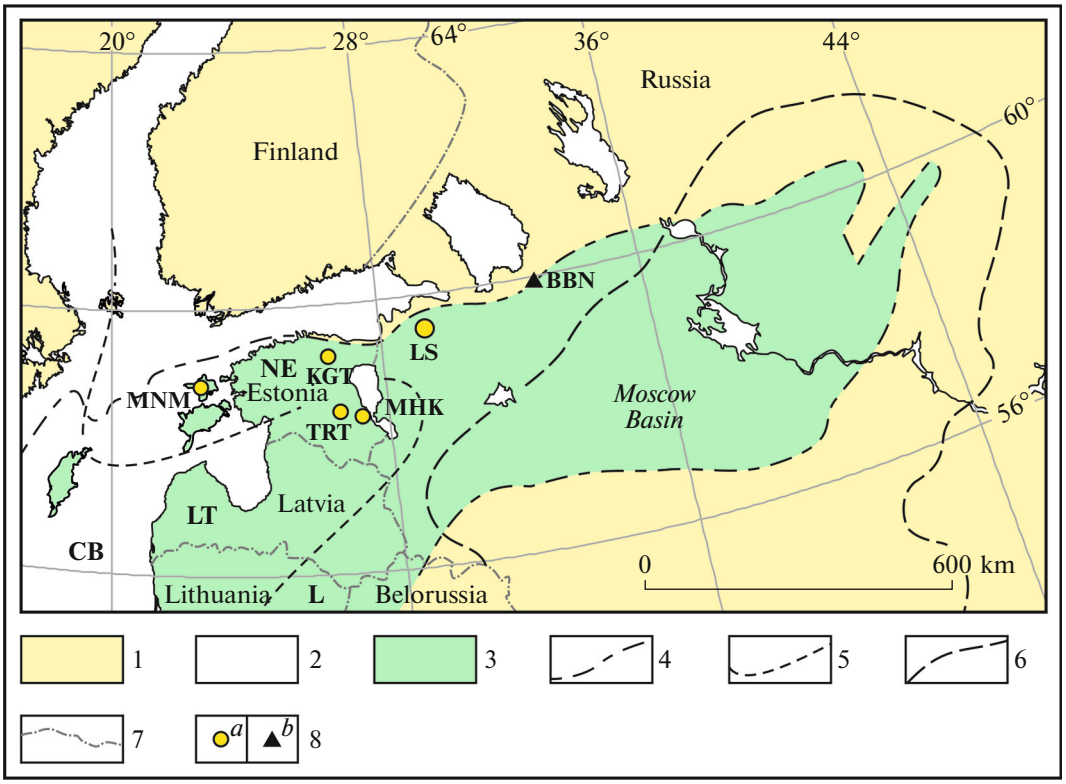
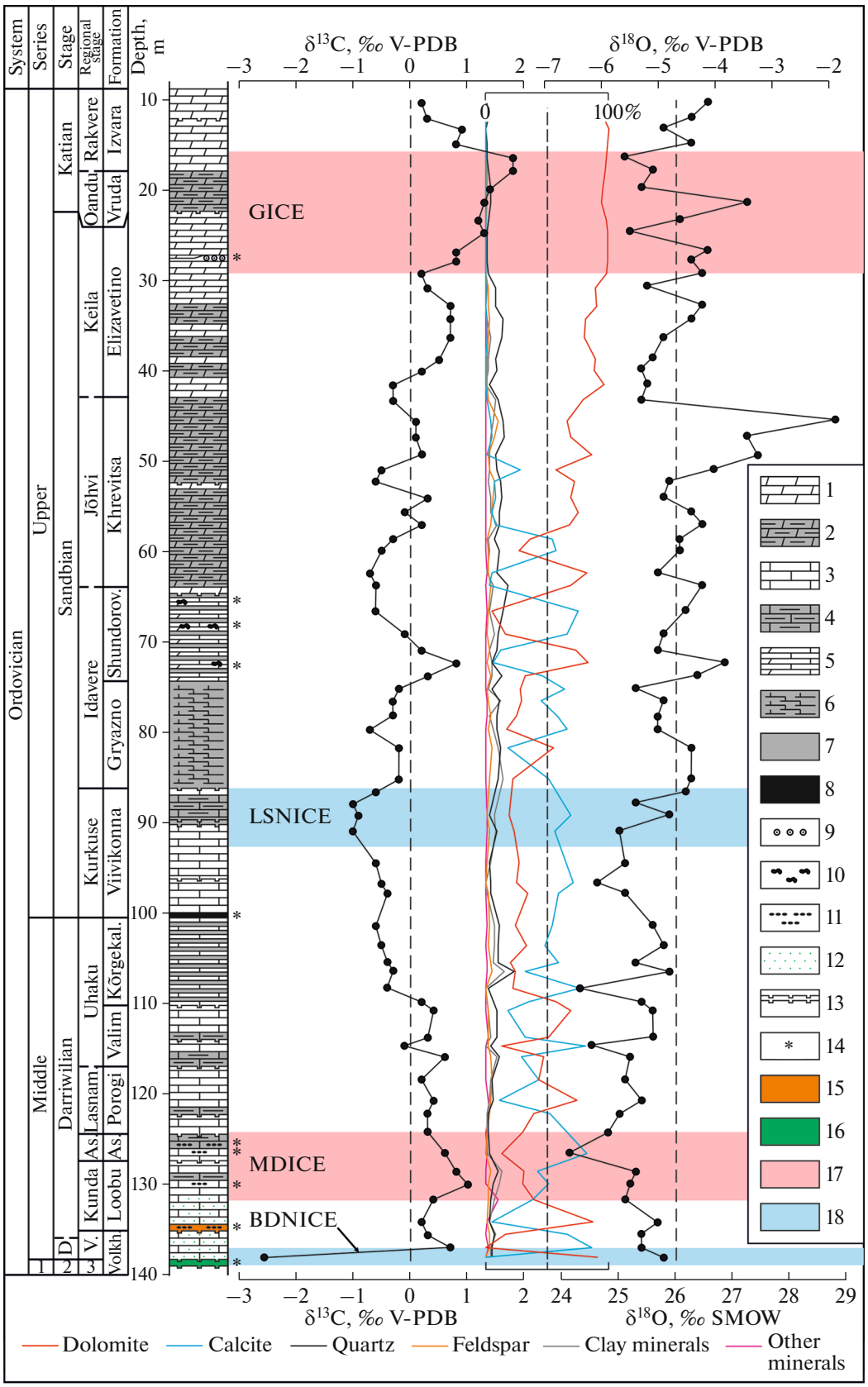


Fig. 1. Schematic geological map of the northwestern Russian Plate showing the distribution of Ordovician deposits and the location of key sections. (1) land; (2) water reservoirs; (3) Ordovician deposits; (4) distribution area of Ordovician rocks; (5) boundaries of facies belts (after Jaanusson, 1995): (NE) North Estonian, (LT) Livonian Trough, (L) Lithuanian, (CB) Central Baltoscandian; (6) outlines of the Moscow Basin; (7) state frontiers; (8) location of sections: boreholes (*a*) and outcrops (*b*): (MNM) Männamaa F-367, (TRT) Tartu-453, (MHK) Mehikoorma-421, (KGT) Kerguta-565, (LS) Lisino-10, (BBN) Babino quarry.

sion is 131 m thick and corresponds to the upper Latorp–lower Rakvere regional stages (Fig. 2). The section of the Lisino-10 borehole is lithologically similar to the sections of North Estonia and can be ascribed to the "transitional" type having much in common with both western (North Estonia) and eastern (Ladoga Klint area) types. This allows a direct lithostratigraphic correlation of its separate intervals with these deposits. Previous biostratigraphic studies of borehole section on acritarchs specified several regional stratigraphic boundaries and allowed the rough biostratigraphic correlation of the Lisino-10 section with some sections of the Baltic region and Moscow basin (Raevskaya and Zaitsev, 2014; Raevskaya and Iskül, 2024). All these facts as well as a continuous core sampling within the Latorp–lower Rakvere interval make the Lisino-10 section a unique object for chemostratigraphic studies and its subsequent correlation with Ordovician sediments of the Baltoscandia and inner regions of the Russian Plate.

This study is aimed at (1) obtaining the continuous C- and O-isotope curves for the carbonate part of the section; (2) studying the mineral composition of carbonate rocks in order to determine their secondary alterations and influence on $\delta^{13}C$ and $\delta^{18}O$ values; (3) identifying chemostratigraphic markers on the obtained carbon isotope curve and their comparison with global isotope events; (4) specifying the age of the Upper Ordovician interval made up of paleontologi-

Fig. 2. Lithological column and variations of carbon ($\delta^{13}C$) and oxygen ($\delta^{18}O$) isotope composition, and mineral composition of carbonate rocks of the Lisino-10 borehole section. (1) dolomites; (2) clayey dolomites; (3) limestones; (4) clayey limestones; (5) alternation of dolomites and limestones; (6) clayey limestones and marls; (7) clay-rich intervals; (8) kukersite; (9) coarse-grained bioclastic material; (10) cherts; (11) ferruginous ooids; (12) glauconite; (13) stratigraphic hiatuses (hardgrounds); (14) off-scale lithological units; (15) informal "lower oolitic bed"; (16) informal "glauconitic sandstone"; (17) Global positive carbon isotope excursions (pink): Middle Darriwilian (MDICE), "Guttenberg" (GICE) carbon isotope events; (18) Global negative carbon isotope excursions (blue): Base-Dapingian (BDNICE), Lower Sandbian (LSNICE). Abbreviations: (D) Dapingian; (V) Volkhov (regional stage); (Volk.) Volkhov (Formation); (As.) Aseri (regional stage), Aseri (Formation); (Lasnam.) Lasnamägi; (Kõrgekal.) Kõrgekallas; (Shundorov.) Shundorovo; (Oand.) Oandu; (Vrud.) Vruda; (Rakver.) Rakvere regional stages: (1) Lower Ordovician, (2) Floia; stage, (3) Latop.


System
Series
Stage
Regional stage
Formation
Depth, m
Ordovician
Upper
Middle
Katian
Sandbian
Darriwilian
Rakvere
Oandu
Keila
Jõhvi
Idavere
Uhaku
Kunda
Loobu
Volkh.
Izvara
Vruda
Elizavetino
Khrevitsa
Shundorov.
Gryazno
Viivikonna
Kõrgekal.
Valim
Porogi
As.
Lasnam.
V.
D
1
2
3
δ13C, ‰ V-PDB
δ18O, ‰ V-PDB
0
100%
GICE
LSNICE
MDICE
BDNICE
δ13C, ‰ V-PDB
δ18O, ‰ SMOW
Dolomite
Calcite
Quartz
Feldspar
Clay minerals
Other minerals

cally poor dolomites; (5) correlation of obtained carbon-isotope curve with previously published data.

GEOLOGICAL OVERVIEW

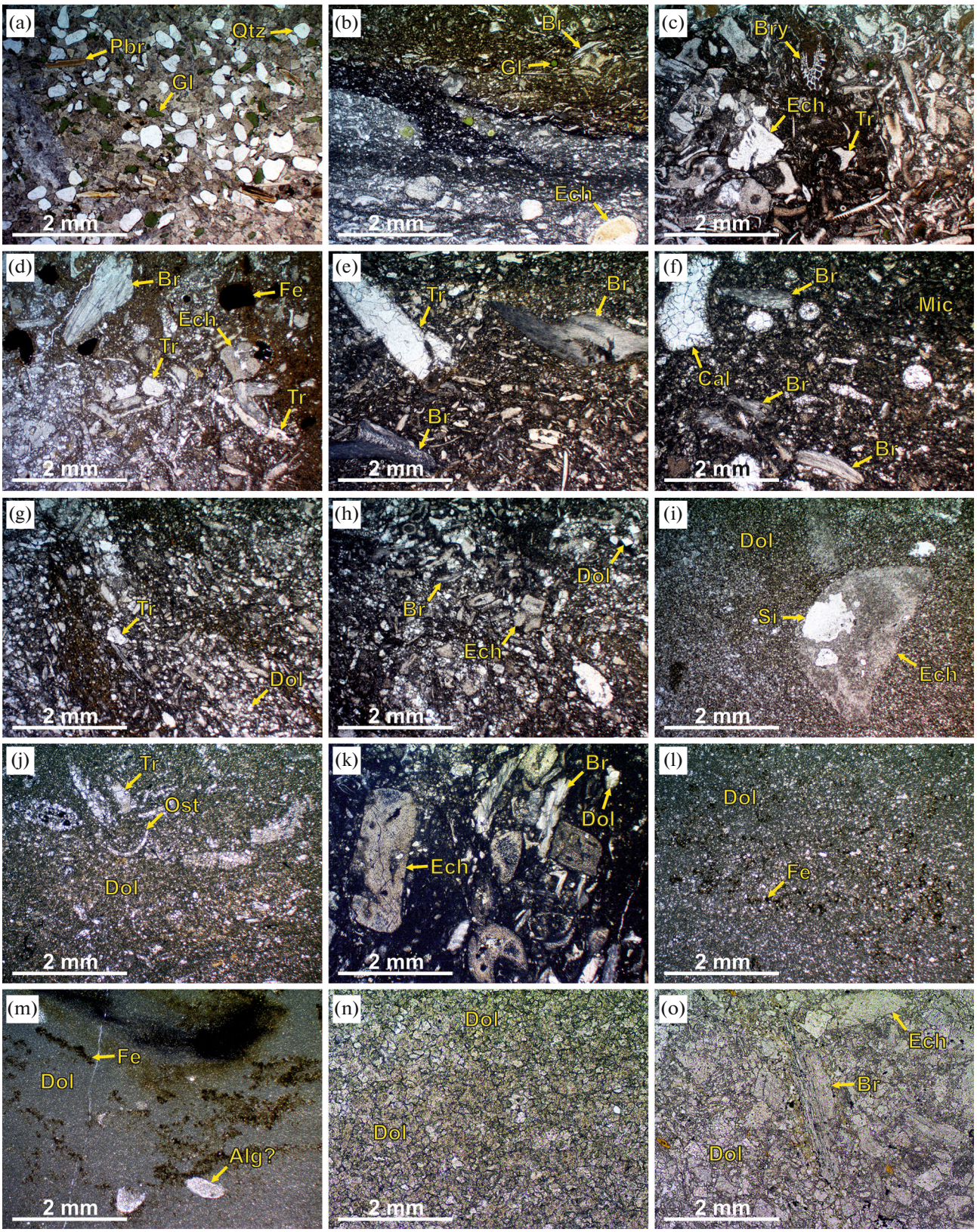
Ordovician rocks are widespread within the Russian Plate and its margins (Fig. 1). In its central part, the Ordovician sediments lie at depths from 1400 to 2400 m and span a significant part of the Moscow basin. The Baltic and Moscow basins are separated by the Lovat swell (Dmitrovskaya, 1993), which was formed in the Late Devonian and serves as a barrier limiting the relations between the western and eastern parts of the basins. At the northeasternmost part of its development area, the Ordovician rocks are exposed as a steep ledge–the Baltic–Ladoga Klint. The Ordovician complex transgressively rests on the different Cambrian stratigraphic levels and is overlain by thin Quaternary (mainly moraine) sediments. In the Southern Baltic area, they are conformably built up by the Lower Silurian. In other cases, they are unconformably overlain by Middle Devonian rocks (Selivanova, 1971). The Ordovician rocks extend latitudinally, forming a low-angle monocline dipping to the south at angles of 0°10′–0°15′ or 2.5–3.5 m for 1 km. The monoclinal bedding is complicated by a gentle isometric undulations, the amplitude of which is no more than 4 m, as well as flexures and NE-trending normal faults with an amplitude of 3–25 m. In some cases, rock bedding is affected by the Quaternary glacial tectonics (Kotlukov and Mitgarts, 1955).

In terms of lithology, Baltoscandian part of the Ordovician basin can be subdivided into facies zones or "belts" (Fig. 1) (Jaanusson, 1995; Männil, 1966; Jaanusson, 1972). The considered section is ascribed to the North Estonian facies belt, which spans the entire area neighboring to the Baltic–Ladoga Klint. In the Klint area of Russia, the Ordovician sections can be conditionally ascribed to two facies types (*Resheniya* ..., 1987). The eastern section type, which includes the Ladoga Klint and the eastern part of the Baltic Klint, consists of relatively deep-water and thick clayey–carbonate deposits. The western facies, including the western part of the Leningrad region and part of North Estonia is characterized by the shallow water condensed carbonate sediments and significant facies differentiation.

The lower part of the studied borehole section (Volkhov, Loobu, Aseri, Porogi, Valim, Kõrgekallas, and Viivikonna formations (Fig. 2)) is composed mainly of dense bioclastic limestones (packstones and wackestones) (Fig. 3). Glauconite (Figs. 3a, 3b) and ferruginous ooids (Fig. 3d) occur at different levels, while the upper parts contain separate layers and admixture of kukersite (Fig. 3g). The middle, more clayey part of the section consists of the Gryazno, Shundorovo, and Khrevitsa formations (Fig. 2). The rocks of the Shundorovo Formation contain remains of siliceous sponges and show mottled silicification (Fig. 3i). The rocks are frequently dolomitized and at some levels are represented by secondary dolomites after bioclastic limestone. Formations that compose this stratigraphic interval have been repeatedly and in detail described in (Põlma, 1982; *Resheniya* ..., 1987; Ivantsov and Melnikova, 2003; *Nizhnii* ... 2012; Dronov et al., 2019, and others), and are not presented in this work.

The upper part of the borehole section is represented by dolomites (Elizavetino, Vruda, and Izvara formations). These formations occur in the south of the Leningrad region and in the northof the Novgorod region, and have no facies analogues in other parts of the basin (*Niznhii* ..., 2012; Verbitsky et al., 2015). In the Klint area of Russia, where formations are fragmentarily exposed, their stratigraphic position remains insufficiently clear (*Nizhnii* ..., 2012]. In the early stratigraphic schemes (Lyutkevich, 1939), this interval of the section was designated as the Kegel regional stage and subdivided into two zones: lower Strophomena asmusi and upper Leperditia ones. In

Fig. 3. Photomicrographs of the main types of carbonate rocks from the Lisino-10 section ($\delta^{13}C$ and $\delta^{18}O$ values are reported in the V-PDB standard): (a, b) Volkhov Formation, (c) Loobu Formation, (d) Aseri Formation, (e) Valim Formation, (f, g) Viivikonna Formation, (h) Gryazno Formation, (i) Shundorovo Formation, (j, k) Khrevitsa Formation, (l) Elizavetino Formation, (m) Vruda Formation, (n, o) Izvara Formation. (a) dolomite with an admixture of quartz, glauconite, and fragments of phosphatic brachiopods (Sample LS10/27-2, $\delta^{13}C = -2.5‰$, $\delta^{18}O = -4.9‰$); (b) bioturbated wackestone with ostracods, brachiopods, and echinoderms (Sample LS10/27-12, $\delta^{13}C = 0.7‰$, $\delta^{18}O = -5.3‰$); (c) trilobite–bryozoan–echinoderm wacke–packstone (Sample LS10/26-32, $\delta^{13}C = 0.4‰$, $\delta^{18}O = -5.6‰$); (d) trilobite–brachiopod–echinoderms wacke-packstone (Sample LS10/25-17, $\delta^{13}C = 0.6‰$, $\delta^{18}O = -6.6‰$); (e) trilobite–brachiopods wackestone (Sample LS10/23-11, $\delta^{13}C = -0.1‰$, $\delta^{18}O = -6.2‰$); (f) trilobite–brachiopod wackestone (Sample LS10/20-33, $\delta^{13}C = -0.5‰$, $\delta^{18}O = -6.1‰$); (g) dolomitic trilobitic wackestone with kukersite (Sample LS10/18-7, $\delta^{13}C = -0.9‰$, $\delta^{18}O = -4.8‰$); (h) brachiopod–echinoderm wacke-packstone (Sample LS10/17-19a, $\delta^{13}C = -0.6‰$, $\delta^{18}O = -4.5‰$); (i) silicified fine-grained dolomite (after wackestone) (Sample LS10/14-3, $\delta^{13}C = 0.8‰$, $\delta^{18}O = -3.8‰$); (j) fine-grained dolomite with quartz admixture (after ostracode–trilobite wackestone) (Sample LS10/11-13, $\delta^{13}C = -0.1‰$, $\delta^{18}O = -4.4‰$); (k) brachiopod–echinoderm wacke-packstone (Sample LS10/10-9, $\delta^{13}C = -0.6‰$, $\delta^{18}O = -4.8‰$); (l) fine-grained, weakly ferruginous dolomite with quartz admixture (Sample LS10/6-5, $\delta^{13}C = 0.7‰$, $\delta^{18}O = -4.2‰$); (m) micro-grained microbial–algal dolomite (Sample LS10/4-20, $\delta^{13}C = 1.4‰$, $\delta^{18}O = -5.3‰$); (n) fine-grained dolomite (Sample LS10/3-3, $\delta^{13}C = 1.8‰$, $\delta^{18}O = -5.6‰$); (o) dolomite (after brachiopod–echinoderm wacke-packstone) (Sample LS10/3-17, $\delta^{13}C = 0.8‰$, $\delta^{18}O = -4.4‰$). Main mineral and biogenic components: (Dol) dolomite, (Qtz) quartz, (Gl) glauconite, (Fe) iron oxides and hydroxides, (Cal) late diagenetic calcite, (Mic) micrite, (Si) chalcedony, (Br) brachiopods, (Pbr) phosphatic brachiopods, (Ech) echinoderms, (Bry) bryozoans, (Tr) trilobites, (Ost) ostracods, (Alg) microbial-algal formations. All photomicrographs are in plane-polarized light.


(a)
Qtz
Pbr
Gl
2 mm
(b)
Br
Gl
Ech
2 mm
(c)
Bry
Ech
Tr
2 mm
(d)
Br
Fe
Ech
Tr
Tr
2 mm
(e)
Tr
Br
Br
2 mm
(f)
Br
Mic
Cal
Br
Br
2 mm
(g)
Tr
Dol
2 mm
(h)
Dol
Br
Ech
2 mm
(i)
Dol
Si
Ech
2 mm
(j)
Tr
Ost
Dol
2 mm
(k)
Br
Dol
Ech
2 mm
(l)
Dol
Fe
2 mm
(m)
Fe
Dol
Alg?
2 mm
(n)
Dol
Dol
2 mm
(o)
Ech
Br
Dol
2 mm

the last version of the Ordovician regional stratigraphic scheme of the western East European Platform, the entire interval was distinguished as the Elizavetino Formation (*Resheniya ...*, 1987). Later, E.Yu. Sammet proposed to preserve name "Elizavetino Formation" only for the lower part of this interval (=Strophomena asmusi zone), while its upper part was divided by him into two new formations: Vruda and Izvara ones (=zone Leperditia) (Verbitsky et al., 2015). Unfortunately, the results of studies by E.Yu. Sammet were not published, while limited data available in the unpublished working geological materials do not provide a reliable insight into the lithological composition of these stratigraphic units. The criteria for distinguishing the Elizavetino, Vruda, and Izvara formations were proposed for the Lisino-10 section by E.G. Raevskaya and G.S. Iskül (Raevskaya and Iskül, 2024) and are used in this work. The borehole section demonstrates continuous succession of these formations, which, based on acritarchs data, correspond to the Keila–lower Rakvere regional stages (Raevskaya and Iskül, 2024). Below, we provide a more detailed description of these units.

Elizavetino Formation (20.9–42.3 m). The stratotype of the Elizavetino Formation is located in the abandoned quarry to the west of the village of Elizavetino (Leningrad region), which gave the name of the formation (*Nizhnii ...*, 2012). In the Lisino-10 section, it is represented by light, pale yellow micro- to fine-grained dolomites (sometimes with relicts of wackestone and packstone structures (Fig. 3l)). The lower part of the formation contains inerlayers of red and light violet micrograined clayey and silty dolomites. The upper part of the Elizavetino Formation consists of microlaminated and wave-laminated dolomites (dolomitic mudstones), frequently with flaser structures and unidentifiable light carbonate laminae supposedly of microbial–algal origin. The thickness is 21.4 m.

Vruda Formation (17.7–20.9 m). The stratotype is located in the abandoned quarry near the Vruda railway station (Leningrad region) (*Nizhnii ...*, 2012). The formation consists of an alternation of brownish and purplish-gray clayey dolomites, dolomitic marls, and micro-grained, usually microlaminated sandy dolomites with desiccation cracks. In the borehole section, the rocks of the Vruda Formation are represented by fine- to micro-grained, frequently clayey dolomites, with indistinct microbial laminae and uneven patchy ferrugination (Fig. 3m). The thickness of the formation in the Lisino-10 borehole is 3.2 m.

Izvara Formation (7.7–17.7 m). The name was given after the village of Izvara in the Volosovo area of the Leningrad region, where its stratotype (recultivated Izvara quarry) is located. The Izvara Formation consists of yellowish micro-grained dolomites, frequently with fenestrae (traces of gas bubbles), desiccation cracks, and pseudomorphs after gypsum. The rocks of this formation also contain an admixture of aeolian quartz sand (Raevskaya and Iskül, 2024). In the Lisino-10 borehole section, the Izvara Formation is incompletely preserved. The lower part of the formation recovered in the borehole consists of micro- and fine-grained mottled (bioturbated?) and flaser-bedded dolomites (Fig. 3n). It occasionally contains interlayers of bioclastic limestone (trilobite–brachiopod–echinoderm wackestone) (Fig. 3o) completely replaced by secondary dolomite. The upper part of the Izvara Formation in the Lisino-10 section has not been preserved; its upper boundary is erosional and is overlain by Quaternary glacial deposits. The thickness of the Izvara Formation in the Lisino-10 section is 10 m.

MATERIALS AND METHODS

In total, 73 carbonate rock samples 0.05–0.1 kg in weight were studied. The lithological composition of the samples was analyzed by optical microscopy in thin section on a Carl Zeiss AxioLab polarization microscope (Geological Institute of the Russian Academy of Sciences) and semiquantitative X-ray powder diffraction at the Laboratory of X-Ray Phase Analysis of the Department of Petroleum Sedimentology and Marine Geology, Geological Faculty of the Moscow State University (Rigaku MiniFlex 600 diffractometer). The percentage proportions of mineral components presented in this work are approximate rather than absolute (Table 1).

The carbon and oxygen isotope composition of carbonates was determined using the Thermoelectron equipment set consisting of the Delta V Advantage mass spectrometer and Gas-Bench-II unit. Carbonates were decomposed in 100% orthophosphoric acid at 50°C. The $\delta^{13}C$ values are given in per mille relative to the V-PDB standard, and $\delta^{18}O$ values are given in per mille relative to V-SMOW, which is related to the V-PDB standard by the formula $\delta^{18}O_{SMOW} = 1.03086 \times \delta^{18}O_{PDB} + 30.86$ (Friedman and O'Neil, 1977). The analysis results are related to V-PDB using calibration samples and IAEA C-O-1 and NBS-19 standards. The accuracy of $\delta^{18}O$ and $\delta^{13}C$ standards is within $\pm 0.2‰$ and $\pm 0.1‰$, respectively.

MINERAL COMPOSITON OF CARBONATE ROCKS

The relative content and distribution of mineral phases in the Ordovician carbonate rocks of the Lisino-10 borehole are shown in Fig. 2. The main mineral components are dolomite and calcite. Calcite has a diverse origin, predominantly biogenic and mechanogenic (bioclasts and their disintegration products). The bioclasts are mainly represented by fragments of articulate brachiopods, trilobites, bryozoans, echinoderms, and other groups of benthic fauna of calcitic composition, as well as skeletal calcareous algae made

Table 1. Isotopic composition ($\delta^{13}C$, $\delta^{18}O$) and semi-quantitative mineralogy of carbonate rocks from the Lisino-10 borehole section

Nos.	Depth, m	Lithology	$\delta^{13}C$ V-PDB	$\delta^{18}O$ V-PDB	$\delta^{18}O$ V-SMOW	Calcite, %	Dolomite, %	Quartz, %	Feldspar, %	Clay minerals, %	Other minerals, %
Izvara Formation											
LS10/2-15	8.8	Dol	0.2	–4.1	26.6	–	99	1	–	–	–
LS10/2-4	10.5	Dol	0.3	–4.4	26.3	–	96	2	2	–	–
LS10/3-27	11.7	Dol	0.9	–4.9	25.8	–	100	–	–	–	–
LS10/3-17	13.4	Dol (Wk)	0.8	–4.4	26.3	–	99	1	–	–	–
LS10/3-3	15.0	Dol	1.8	–5.6	25.1	–	98	1	1	–	–
Vruda Formation											
LS10/4-39	16.4	Dol	1.8	–5.1	25.6	–	97	2	1	–	–
LS10/4-20	18.4	Dol (Md)	1.4	–5.3	25.4	–	95	4	1	–	–
LS10/4-9	20.0	Dol (Md)	1.3	–3.5	27.3	–	94	4	1	1	–
Elizavetino Formation											
LS10/5-39	22.0	Dol (Md)	1.2	–4.6	26.1	–	98	2	–	–	–
LS10/5-31	23.3	Dol (Md)	1.3	–5.5	25.2	–	99	1	–	–	–
LS10/5-9	25.5	Dol	0.8	–4.1	26.6	–	99	1	–	–	–
LS10/5-24	26.6	Dol	0.8	–4.4	26.3	–	99	1	–	–	–
LS10/6-35	28.0	Dol (Md)	0.2	–4.2	26.5	–	98	2	–	–	–
LS10/6-17	29.6	saDol	0.3	–5.2	25.5	–	89	8	2	1	–
LS10/6-5	31.7	saDol	0.7	–4.2	26.5	–	90	8	2	–	–
LS10/7-30	33.1	saDol	0.7	–4.4	26.3	1	81	14	3	1	–
LS10/7-17	35.2	saDol	0.7	–4.9	25.8	1	80	13	2	4	–
LS10/7-4	37.6	saDol (Wk)	0.5	–5.1	25.6	–	89	8	1	2	–
LS10/8-24	38.9	Dol (Wk)	0.2	–5.3	25.4	–	88	9	1	2	–
LS10/8-14	40.5	Dol (Wk)	–0.3	–5.2	25.5	–	96	3	1	–	–
Khrevitsa Formation											
LS10/8-6	42.2	saDol (Wk)	–0.3	–5.3	25.4	1	79	10	2	8	–
LS10/9-17a	44.6	Dol (Wk)	0.1	–1.9	28.9	4	66	14	10	6	–
LS10/9-12	46.4	Dol (Wk)	0.1	–3.5	27.3	5	69	15	7	4	–
LS10/9-1	48.4	Dol (Wk)	0.2	–3.3	27.5	1	86	8	2	3	–
LS10/10-13	50.1	Dol (Wk)	–0.5	–4.0	26.7	28	57	9	3	3	–
LS10/10-9	51.4	Dol (Wk)	–0.6	–4.8	25.9	7	72	12	7	2	–

Table 1. (Contd.)

Nos.	Depth, m	Lithology	$\delta^{13}C$ V-PDB	$\delta^{18}O$ V-PDB	$\delta^{18}O$ V-SMOW	Calcite, %	Dolomite, %	Quartz, %	Feldspar, %	Clay minerals, %	Other minerals, %
LS10/10-1	53.2	Dol (Wk)	0.3	–4.9	25.8	8	69	13	6	4	–
LS10/11-13	54.9	saDol (Wk)	–0.1	–4.4	26.3	5	75	11	5	4	–
LS10/11-7	56.3	dolWk	0.2	–4.2	26.5	8	68	11	4	9	–
LS10/11-1	57.9	dolWk	–0.3	–4.6	26.1	54	36	7	1	2	–
LS10/12-14	59.2	dolWk	–0.5	–4.6	26.1	57	27	11	2	3	–
LS10/12-4	61.7	dolWk	–0.7	–5.0	25.7	5	82	9	2	1	1
Shundorovo Formation											
LS10/13-20	63.1	silDol(Wk)	–0.6	–4.2	26.5	3	69	18	4	6	–
LS10/13-9	66.0	saWk	–0.6	–4.5	26.2	75	5	14	2	3	1
LS10/14-15	68.6	sa-dolWk	–0.1	–4.9	25.8	66	16	10	1	7	–
LS10/14-8	70.4	saDol (Wk)	0.2	–5.0	25.7	12	73	9	3	3	–
LS10/14-3	71.8	silDol (Wk)	0.8	–3.8	26.9	6	83	5	1	5	–
LS10/15-15	73.3	sa-dolWk	0.3	–4.3	26.4	46	32	13	4	5	–
Gryazno Formation											
LS10/15-7	74.8	sil-dolWk	–0.2	–5.4	25.3	64	28	5	1	2	–
LS10/15-5	76.1	sa-dolWk	–0.3	–4.9	25.8	45	29	11	2	12	1
LS10/16-6	77.8	sa-dolWk	–0.3	–5.0	25.7	58	25	9	4	3	1
LS10/16-16	79.3	sa-dolWk	–0.7	–5.0	25.7	66	17	9	2	6	–
LS10/16-22	81.4	silDol (Md)	–0.2	–4.4	26.3	18	55	12	5	10	–
LS10/17-14	84.9	sa-dolWk	–0.2	–4.4	26.3	51	22	10	3	14	–
LS10/17-19a	86.4	dolWk–dolPk	–0.6	–4.5	26.2	70	21	5	1	2	1
Viivikonna Formation											
LS10/18-11	87.7	Wk	–1.0	–5.4	25.3	42	45	7	3	2	1
LS10/18-7	89.0	dolWk	–0.9	–4.8	25.9	69	19	3	1	7	1
LS10/18-3	90.8	dolLs	–1.0	–5.7	25.0	56	23	9	3	8	1
LS10/19-11	94.3	dolLs	–0.6	–5.6	25.1	65	27	3	1	4	–
LS10/20-44	96.6	dolWk	–0.5	–6.1	24.6	71	25	4	–	–	–
LS10/20-33	97.8	dolWk	–0.4	–5.6	25.1	59	34	4	2	1	–

Table 1. (Contd.)

Nos.	Depth, m	Lithology	$\delta^{13}C$ V-PDB	$\delta^{18}O$ V-PDB	$\delta^{18}O$ V-SMOW	Calcite, %	Dolomite, %	Quartz, %	Feldspar, %	Clay minerals, %	Other minerals, %
Kõrgekallas Formation											
LS10/20-12	101.4	sa-dolWk	–0.6	–5.1	25.6	54	24	11	3	7	1
LS10/21-32	103.7	sa-dolWk	–0.5	–4.9	25.8	48	33	10	2	7	–
LS10/21-21	105.6	sa-dolWk	–0.4	–5.4	25.3	59	20	10	4	6	1
LS10/21-11	106.6	sa-dolWk	–0.3	–4.8	25.9	32	24	23	5	15	1
LS10/22-30	108.5	dolWk	–0.4	–6.4	24.3	76	22	2	–	–	–
LS10/22-16	110.0	Dol (Wk)	0.2	–5.3	25.4	35	57	6	1	1	–
Valim Formation											
LS10/22-10	111.0	saDol (Wk)	0.4	–5.1	25.6	18	69	9	2	2	–
LS10/23-3	114.0	saDol (Wk)	0.3	–5.1	25.6	32	51	9	2	4	2
LS10/23-11	115.0	dWk–dPk	–0.1	–6.2	24.5	81	13	4	2	–	–
LS10/23-18	116.2	saDol (Wk)	0.6	–5.5	25.2	29	47	11	4	9	–
Porogi Formation											
LS10/23-37	118.8	dWk–dPk	0.2	–5.6	25.1	43	43	5	5	4	–
LS10/24-23	121.1	Dol (Wk)	0.4	–5.3	25.4	11	74	6	4	3	2
LS10/24-13	122.6	dPk	0.3	–5.7	25.0	52	39	2	3	1	3
LS10/25-25	124.7	dPk	0.3	–5.9	24.8	66	30	2	1	1	–
Aseri Formation											
LS10/25-17	127.1	dWk–dPk	0.6	–6.6	24.1	82	13	3	–	1	1
Loobu Formation											
LS10/25-7	129.1	dolLs	0.8	–5.4	25.3	42	31	10	4	13	–
LS10/26-42	130.5	dWk–dPk	1.0	–5.5	25.2	51	30	6	2	11	–
LS10/26-32	132.3	dPk	0.4	–5.6	25.1	38	39	4	2	7	10
LS10/26-12	134.8	Dol	0.2	–5.0	25.7	5	87	3	1	3	1
Volkhov Formation											
LS10/27-23	136.2	dolLs	0.3	–5.3	25.4	66	16	7	3	8	0
LS10/27-12	137.7	q-glWk	0.7	–5.3	25.4	86	–	5	3	4	2
LS10/27-2	138.8	q-glDol	–2.5	–4.9	25.8	–	91	5	–	4	–

Dol—dolomite; Dol (Wk)—dolomite after wackestone; Dol (Md)—dolomite after mudstone; Wk—wackestone; Pk—packstone; Wk–Pk—wacke-packstone; Ls—limestone. Components: sa—sandy; dol—dolomitic; sil—silicified; q-gl—quartz-glauconitic.

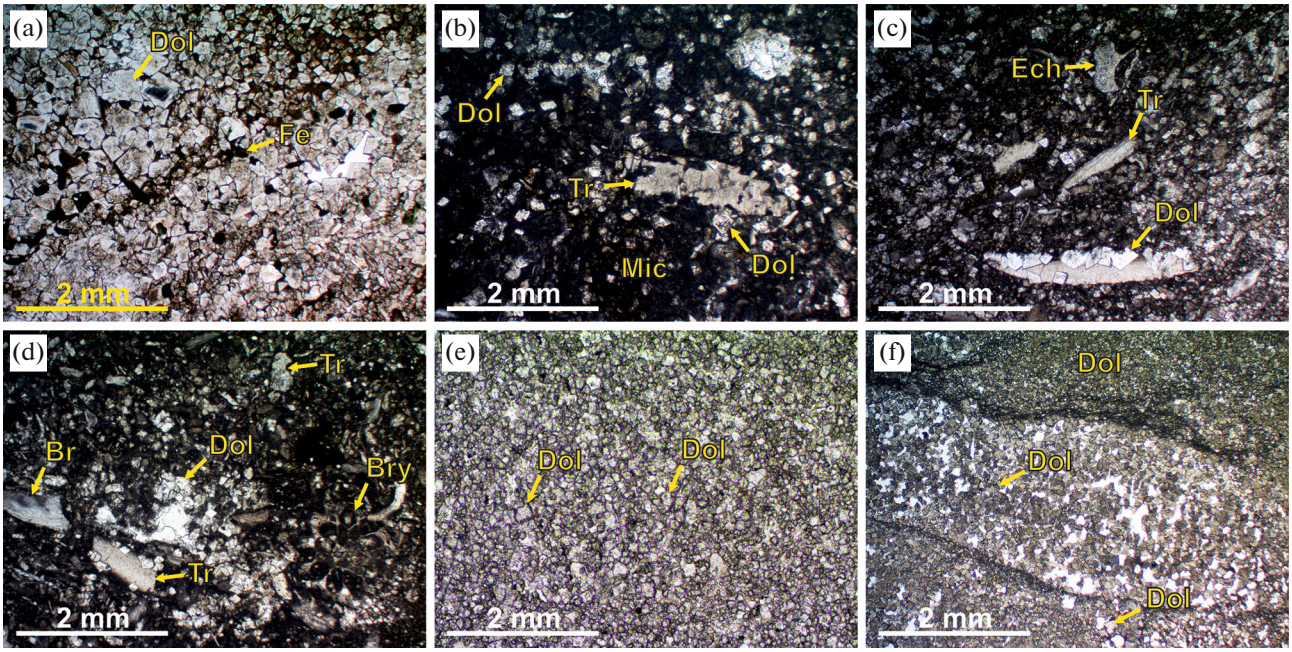


Fig. 4. Photomicrographs of the main types of dolomite from the Lisino-10 section ($\delta^{13}C$ and $\delta^{18}O$ values are reported in the V-PDB standard). (a) xenomorphic (anhedral) dolomite with areas of hypidiomorphic (subhedral) dolomite, the lower part of the Loobu Formation (Sample LS10/26-12, $\delta^{13}C = 0.2‰$, $\delta^{18}O = -5.0‰$); (b) euhedral dolomite crystals, the lower part of the Kõrgekallas Formation (Sample LS10/22-30, $\delta^{13}C = -0.4‰$, $\delta^{18}O = -6.4‰$); (c) euhedral dolomite with a minor admixture of subhedral crystals, the lower part of the Viivikonna Formation (Sample LS10/20-44, $\delta^{13}C = -0.5‰$, $\delta^{18}O = -6.1‰$); (d) hypidiomorphic (subhedral) dolomite, the lower part of the Gryazno Formation (Sample LS10/17-19a, $\delta^{13}C = -0.6‰$, $\delta^{18}O = -4.5‰$); (e) hypidiomorphic (subhedral) dolomite, the base of the Shundorovo Formation (Sample LS10/15-15, $\delta^{13}C = 0.3‰$, $\delta^{18}O = -4.3‰$); (f) hypidiomorphic (subhedral) and xenomorphic (anhedral) dolomite, upper part of the Izvara Formation (Sample LS10/2-15, $\delta^{13}C = 0.2‰$, $\delta^{18}O = -4.1‰$). Main mineral and biogenic components shown in Fig. 3. All photomicrographs are in plane-polarized light.

up of magnesian calcite (Fortunatova et al., 2005; Korobov et al., 2018). Chemogenic calcite is mainly represented by micrite (microgranular crystalline calcite), which usually forms the rock matrix. Secondary micro- to fine-grained sparitic calcite is present as an admixture in the clayey–micritic or dolomitic matrix and more rarely encrusts the bioclasts of echinoderms or brachiopods. Dolomite usually has a micro to fine-grained texture and consists of hypidiomorphic (subhedral), or, more rarely, euhedral crystals (Gregg and Sibley, 1984; Zhemchugova and Maslova, 2002). Micrograined varieties with xenomorphic (anhedral) crystals occur at some levels (Loobu and Viivikonna formations). The Mg-calcite identified in some samples was not considered separately. It is usually restricted to the intervals with euhedral dolomite.

The lower part of the section is represented by the Volkhov and Valim formations and has an average dolomite content of about 40%, reaching 70% in isolated samples. The rocks consist of bioclastic limestones (wackestones and packstones), more rarely dolomites (Fig. 4a).

The Kõrgekallas (Fig. 4b) and Viivikonna (Fig. 4c) formations are represented by weakly altered (dolomitized) wackestones. The rocks of this interval have an approximately equal content of dolomite (around 30%). The dolomite is represented by euhedral grains.

The Gryazno–lower Khrevitsa interval is characterized by wave-like variations and a negative correlation of dolomite and calcite (with component contents averaging about 40%). The dolomite maximum is correlated with the minimum content of calcite. The micro- to fine-grained, subhedral dolomite mainly replaces the clayey–micritic rock matrix (Figs. 4d, 4e).

The upper part of the section, which includes almost the entire Khrevitsa, Elizavetino, Vruda, and Izvara formations, is composed of micro- to fine-grained dolomites. A significant amount of calcite was found only in the interval of the Khrevitsa Formation, where its average content usually does not exceed 10%. The morphology of dolomite grains corresponds to the hypidiomorphic (subhedral) and xenomorphic (anhedral) types (Fig. 4f).

Clay minerals in the studied rocks are represented by mica and chlorite. Their total content throughout the entire studied section is usually no more than 10%, reaching 30–40% at some levels of the Loobu, Kõrgekallas, and Gryazno formations (Fig. 2). The coarser-grained (silty and sandy) terrigenous material is represented by quartz and feldspars, and their total

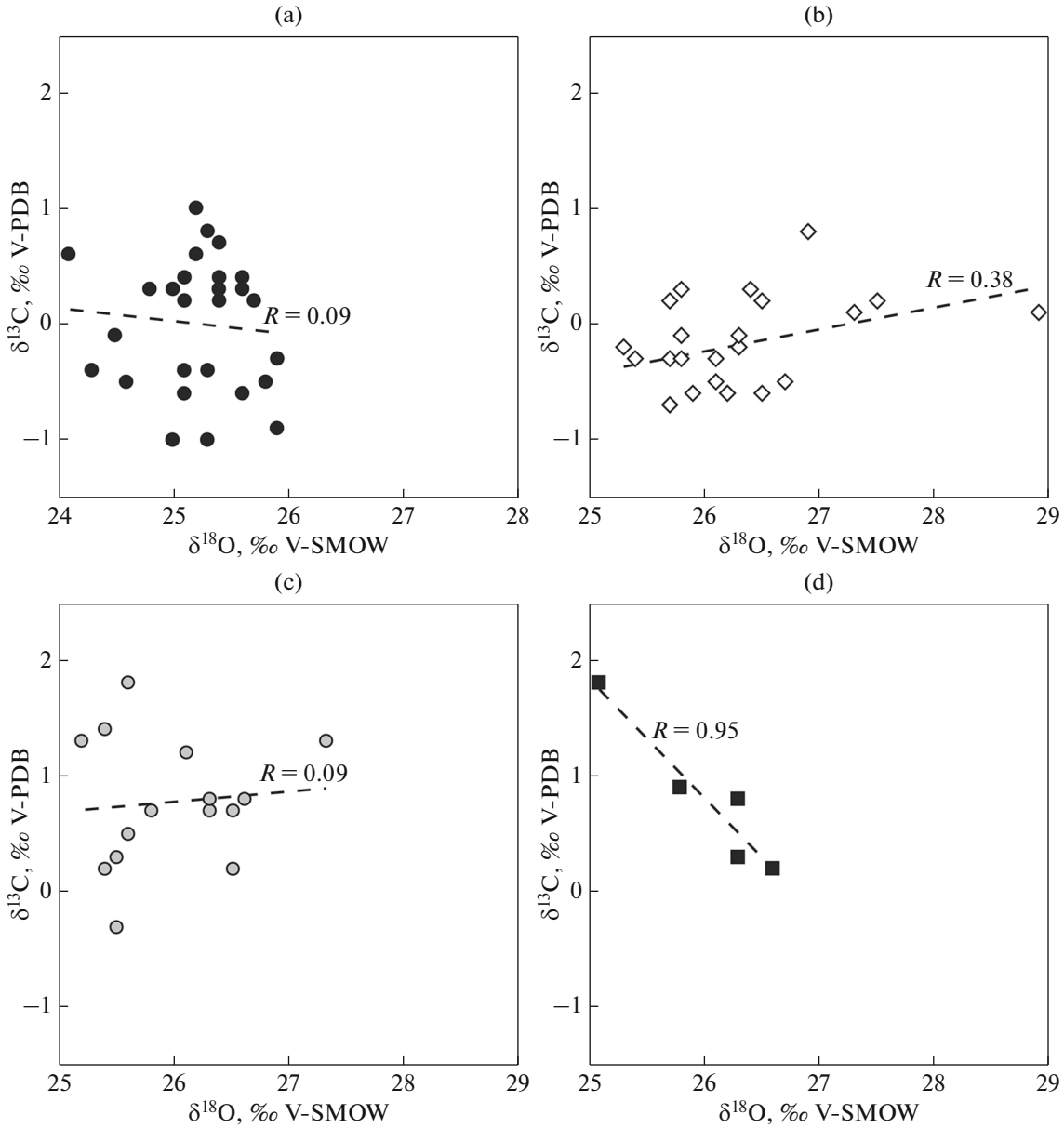


Fig. 5. Variations of carbon (V-PDB) and oxygen (V-SMOW) isotope compositions in the carbonates of the Lisino-10 borehole. (a) Volkhov–Viivikonna formations (Dapingian–Lower Sandbian stages), (b) Gryazno, Shundorovo and Khrevitsa formations (middle part of the Sandbian Stage), (c) Elizavetino and Vruda formations (Upper Sandbian–base of the Katian Stage), (d) Izvara Formation (Katian Stage).

amount rarely exceeds 10%. In general, the total content of terrigenous admixture in the carbonate component of the Lisino-10 section is insignificant and does not show any sharp variations. Authigenic minerals are represented by siderite, apatite, goethite, and pyrite occur in accessory amounts (less than 10%).

RESULTS OF ISOTOPE STUDIES

The carbon and oxygen isotope composition was analyzed in 73 whole-rock carbonate samples spanning the stratigraphic interval of the Volkhov–Izvara formations (Latorp–lower Rakvere regional stages (Fig. 2)). A total scatter of $\delta^{13}C$ values varies from –2.5 to 1.8‰. In general, the borehole section is characterized by the upsection $\delta^{13}C$ depletion of carbonates from the lower part of the Volkhov Formation to the base of the Gryazno Formation, and then by a gradual $\delta^{13}C$ enrichment to the base of the Izvara Formation (Table 1). The widest $\delta^{13}C$ variations occur in the upper Ordovician (Gryazno–Izvara formations). The minimum $\delta^{13}C = -2.5$‰ was found in the lowermost sample (lower parts of the Dapingian Stage, Latorp

regional stage, Volkhov Formation). The ^{18}O values fall between 24.1 and 28.9‰ and are characterized by significant variations at total upsection increase (Table 1).

Based on the carbon isotope composition, the borehole section can be subdivided into four intervals: (1) lower interval corresponding to the entire Middle Ordovician, including the lowermost part of the Upper Ordovician (Volkhov–Viivikonna formations); (2) the Gryazno, Shundorovo, and Khrevitsa formations (Sandbian Stage); (3) interval including the uppermost part of the Sandbian Stage and the lowermost part of the Katian Stage (Elizavetino and Vruda formations); (4) the Izvara Formation (lower part of the Katian Stage).

The lower interval including the Lower–Middle Ordovician (Dapingian–Darriwilian stages, Volkhov–Kõrgekallas formations) and lower Upper Ordovician (Sandbian Stage, Viivikonna Formation) is characterized by $\delta^{13}C$ values varying between −1.0 and 1.0‰ ($C_{av} = 0.2 \pm 0.6$‰). Upsection, the $\delta^{13}C$ values show a gradual decrease from 1.0‰ in the upper part of the Loobu Formation to −1.0‰ in the upper boundary of the Viivikonna Formation. The $\delta^{18}O$ values in this interval vary in a relatively narrow range from 24.1 to 25.9‰ ($O_{av} = 25.3 \pm 0.4$‰). Correlation between $\delta^{13}C$ and $\delta^{18}O$ values is absent ($R = 0.09$, Fig. 5a).

The rocks of the Gryazno, Shundorovo, and Khrevitsa formations are characterized by more diverse, predominantly negative $\delta^{13}C$ values (−0.7...0.8‰), which on average (-0.2 ± 0.4‰) are 0.4‰ lower than values in the underlying interval. The positive $\delta^{13}C$ values are confined to the base of the Shundorovo Formation and two levels in the middle (0.2...0.3‰) and upper (0.1...0.2‰) parts of the Khrevitsa Formation. On the carbon isotope curve, these levels correspond to three moderate-amplitude (0.7...1.4‰) positive excursions, the highest amplitude of which (1.4‰) was found at the base of the Shundorovo Formation. In contrast to the carbon isotope composition, the oxygen isotope values show significant $\delta^{18}O$ variations, which fall in the interval from 25.3 to 28.9‰ ($O_{av} = 26.2 \pm 0.8$‰). The oxygen-isotope curve demonstrates several moderate and high-amplitude positive $\delta^{18}O$ excursions (up to 3.5‰), which coincide with positive $\delta^{13}C$ anomalies. The highest amplitude positive oxygen isotope excursion (3.5‰) is restricted to the upper part of the Khrevitsa Formation and coincides with the moderate-amplitude positive spike on the carbon isotope curve. In general, the considered interval is characterized by simultaneous upsection increase of the carbon and oxygen isotope compositions, which is confirmed by the correlation between $\delta^{13}C$ and $\delta^{18}O$ ($R = 0.38$, Fig. 5b).

The interval comprising the deposits of the Elizavetino and Vruda formations corresponds to the boundary sediments of the Sandbian and Katian stages. It is mainly characterized by positive $\delta^{13}C$ values from 0.2 to 1.8‰ ($C_{av} = 0.7 \pm 0.5$‰). Against the background of the general upsection increase of carbon isotope composition, two negative excursions with an amplitude of around 0.5‰ are distinguished in the lower and middle parts of the Elizavetino Formation. The $\delta^{18}O$ values in this interval vary from 25.4 to 27.3‰ ($O_{av} = 25.8 \pm 0.6$‰) and show significant variability in the upper part of this interval. Like the carbon isotope curve, the $\delta^{18}O$ curve shows an upsection increase. The correlation between $\delta^{18}O$ and $\delta^{13}C$ is absent due to frequent random variations of $\delta^{18}O$ ($R = 0.09$, Fig. 5c).

In the sediments of the Izvara Formation, the $\delta^{13}C$ values are positive and range from 0.2 to 1.8‰ ($C_{av} = 0.8 \pm 0.6$‰). These values show an upsection decrease. The $\delta^{18}O$ values range from 25.1 to 26.6‰ ($O_{av} = 26.3 \pm 0.6$‰). In contrast to the carbon isotope composition, $\delta^{18}O$ values gradually increase upsection. This interval is characterized by a distinct negative correlation between $\delta^{13}C$ and $\delta^{18}O$ ($R = -0.95$, Fig. 5d).

DISCUSSION

Stages of Dolomite Formation

The entire studied stratigraphic interval shows varying degrees of dolomitization (Fig. 2). Based on the morphology and texture, four types of dolomites are distinguished: (1) an early type, occurring as isolated micro- to fine-grained euhedral rhombic crystals confined to the clayey–micritic rock matrix (Fig. 4b); (2) hypidiomorphic (subhedral), fine- to medium-grained dolomite (Figs. 4d, 4e), which completely or partly replaces the clayey–carbonate matrix and frequently contains inclusions of clayey material; (3) late diagenetic dolomite represented by subhedral, more rarely xenomorphic anhedral crystals (Fig. 4f); (4) a possibly epigenetic dolomite, observed in various parts of the section, consisting of medium- to coarse-grained xenomorphic crystals that often form a "mosaic" texture (Põlma, 1982).

The dolomites of the Elizavetino, Vruda, and Izvara formations (Fig. 4f) are composed mainly of hypidiomorphic micro- to fine-grained crystals of type 2. These dolomites are characterized by fine lamination, desiccation cracks, and pseudomorphs after gypsum crystals (Raevskaya and Iskül, 2024), as well as the heavier $\delta^{13}C$ composition, which may indicate formation in an evaporitic basin under shallow subsurface conditions typical of a sabkha setting (Dronov and Holmer, 1999; Dronov and Rozhnov, 2007; Liang et al., 2023).

Dolomite of type 3 is confined to the intervals that, on macro- and microscales, show the predominance of skeletal calcareous algae of the aragonite or high-Mg calcitic composition, which have higher solubility

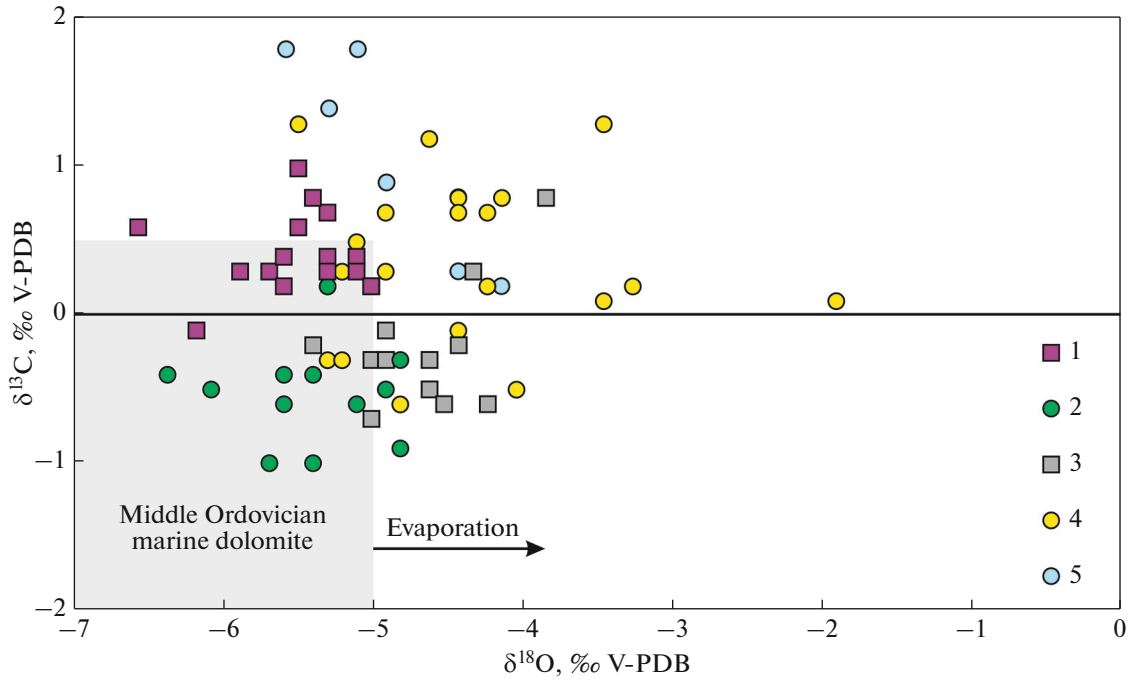


Fig. 6. Carbon and oxygen isotope composition ($\delta^{13}C$ vs. $\delta^{18}O$, V-PDB) of dolomites from the Lisino-10 section. (1) Volkhov–Valim formations, (2) Kõrgekallas–Viivikonna formations, (3) Gryazno–lower part of the Khrevitsa Formation, (4) middle and upper parts of the Khrevitsa–Elizavetino formations, (5) Vruda and Izvara formations.

(Maslov, 1956, 1961; Fortunatova et al., 2005; Korobov et al., 2018). Most of the thin algal skeletons likely dissolved soon after accumulation on the seafloor or during early diagenesis, which led to the enrichment of pore waters in Mg^{2+}. Mixing of solutions with different electrolyte concentrations can lead to either precipitation or dissolution of sediment (Leeder, 1986). According to this model, mixing of predominantly fresh meteoric waters with about 30% seawater causes calcite undersaturation, whereas dolomite saturation increases. Thus, the presence of 5–30% seawater in solution will lead to either calcite replacement by dolomite or primary precipitation of dolomite. This process is common in ancient rocks associated with the retrograde sedimentation, which led to the subsequent formation of dolomite of types 1–3.

The later (possibly epigenetic) dolomitization may be related to burial of the rock to significant depths, with subsequent downward infiltration of bottom waters of elevated salinity, which, under elevated pressure and temperature conditions, facilitated the formation of type 4 dolomite and the formation of a "mosaic" texture of the rock (Bai et al., 2016).

Post-depositional Isotope Alterations

Diagenetic alterations of isotope composition are often manifested as a positive correlation between $\delta^{13}C$ and $\delta^{18}O$ values. Significant $\delta^{18}O$ variations unrelated to a change of lithological composition could result from both interaction with heavy oxygen-depleted meteoric waters during sedimentation and from post-depositional processes (Pokrovsky et al., 2021, 2022; Veizer et al., 1999). Petrographic examination of thin sections revealed that the most significant post-depositional transformations are expressed as several phases of dolomitization that occurred at the early and middle diagenetic stages (see above). The $\delta^{13}C$ and $\delta^{18}O$ values in most of the studied samples (Fig. 5) are lower than those of Ordovician brachiopods shells that have been carefully screened and are considered "reference" values for open-marine basins (Veizer et al., 1999). At the same time, most of the isotope values for the Lower–Middle Ordovician dolomites from the Lisino-10 section fall within the field corresponding to the isotopic composition of marine Ordovician dolomites (Fig. 6) (Bai et al., 2016). The isotope composition of primary sedimentary dolomites is often better preserved than that of the associated limestones, which is explained by their lower solubility during postdiagenetic processes (Melezhik et al., 2005; Pokrovsky et al., 2021). Likely, the sediments could be subjected to crystallization already at the early diagenetic stages in an open water–sediment system (Huang et al., 2021). Thus, the isotope composition of pore and bottom waters was similar (Veizer et al., 1999).

The main factor affecting the postdiagenetic alterations of $\delta^{13}C$ and $\delta^{18}O$ composition is rock interaction with groundwaters (Pokrovsky et al., 2021). These

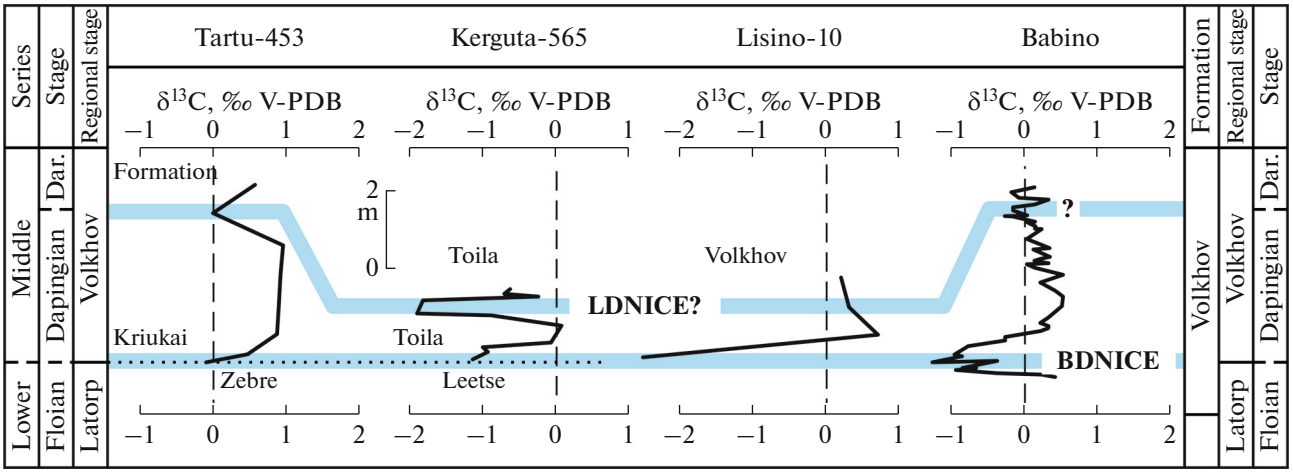


Fig. 7. Correlation of carbon isotope ($\delta^{13}C$) curves across the Floian, Dapingian, and Darriwilian boundary interval in the Lisino-10 section with published data from: Tartu-453 borehole (Bauert et al., 2014), Kerguta-565 borehole (Kaljo et al., 2007), and Babino quarry (Zaitsev and Pokrovsky, 2014). Abbreviations: (Dar.) Darriwilian.

transformations are mainly caused by the presence of organic matter (OM) (Saltzman and Thomas, 2012) and by elevated temperatures associated with burial depths (Veizer et al., 1999; Pokrovsky et al., 2021, 2022). The $\delta^{18}O$ values (24.1...28.9‰, O_{av} = 25.8 ± 0.7‰) obtained from the Lisino-10 borehole section are much higher than those accepted as boundary values ($\delta^{18}O$ = 20.5‰ SMOW) between the altered and unaltered Early Paleozoic carbonates (Pokrovsky et al., 2022; Veizer et al., 1999), which is inconsistent with a significant subsidence of the studied rocks.

A negative correlation between carbon and oxygen isotope compositions established in the carbonates of the Izvara Formation (Fig. 5d) is likely unrelated to the post-depositional modifications and was caused by the superposition of unrelated events: a "local" event that reduced the supply of clay components carrying ^{18}O-depleted terrigenous material to the precipitating sediments and a "global" event marking the GICE completion.

Isotope Correlation and Nature of Carbon–Isotope Excursions

Isotope studies of the Lisino-10 borehole section have identified four carbon isotope events, which correspond to the stratigraphic interval from Floian to the lower Katian stages (Fig. 2). Two positive excursions can be confidently correlated with the MDICE and GICE excursions of the global Ordovician carbon isotope curve (Bergström et al., 2009a). Negative excursions confined to the base of the Dapingian Stage (BDNICE) and the lower part of the Sandbian Stage (LSNICE excursion) can be regarded as additional stratigraphic markers. A negative excursion at the base of the Darriwilian Stage (LDNICE, Lower Darriwilian Negative Isotopic Carbon Excursion) in the Lisino-10 borehole section was supposedly recorded in the upper part of the Volkhov Formation (Fig. 7). On the $\delta^{13}C$ curve of the Lisino-10 borehole, this excursion is very weakly expressed (~0.5‰) and can be detected only through detailed correlation of carbon isotope curves. Therefore, it is not discussed in detail within the scope of this study.

A negative carbon isotope excursion at the base of the Dapingian Stage, BDNICE, was found in many regions worldwide: in Sweden (Lehnert et al., 2014), North Estonia (Kaljo et al., 2007), Argentine Precordillera (Buggisch et al., 2003; Albanesi et al., 2006), USA (Edwards and Saltzman, 2014), China (Munnecke et al., 2011; Wang et al., 2009), on the Siberian Platform (Pokrovsky et al., 2018), and others. In the Ordovician rocks of the northwestern Russian Plate, it was first documented in the Babino section at the base of the Volkhov Formation (Zaitsev and Pokrovsky, 2014). In the Lisino-10 section, this excursion was recorded in one sample (Fig. 2), where its visible amplitude is about 2.5–3‰. In the section of the Babino quarry, this excursion is slightly lower (~2‰), but the rocks of this section have the lighter (by 0.5–1‰) $\delta^{13}C$ and $\delta^{18}O$ isotope composition (Fig. 7), which is likely due to the deeper-water depositional environment of these rocks.

It is suggested that the positive $\delta^{13}C$ excursions correspond to the episodes of high bioproductivity when the sedimentary conditions favored OM burial in the sediments (Kump, 2003). Negative deviations of $\delta^{13}C$ isotope composition, in contrast, reflect the periods of decreased bioproductivity and/or reduced OM burial. In the northwestern Russian Plate, the Floian–Dapingian boundary corresponded to shallow-water environments with greatly reduced carbonate sedimentation and active hydrodynamics (Dronov, 1998; Dronov et al., 1998), which facilitated the formation

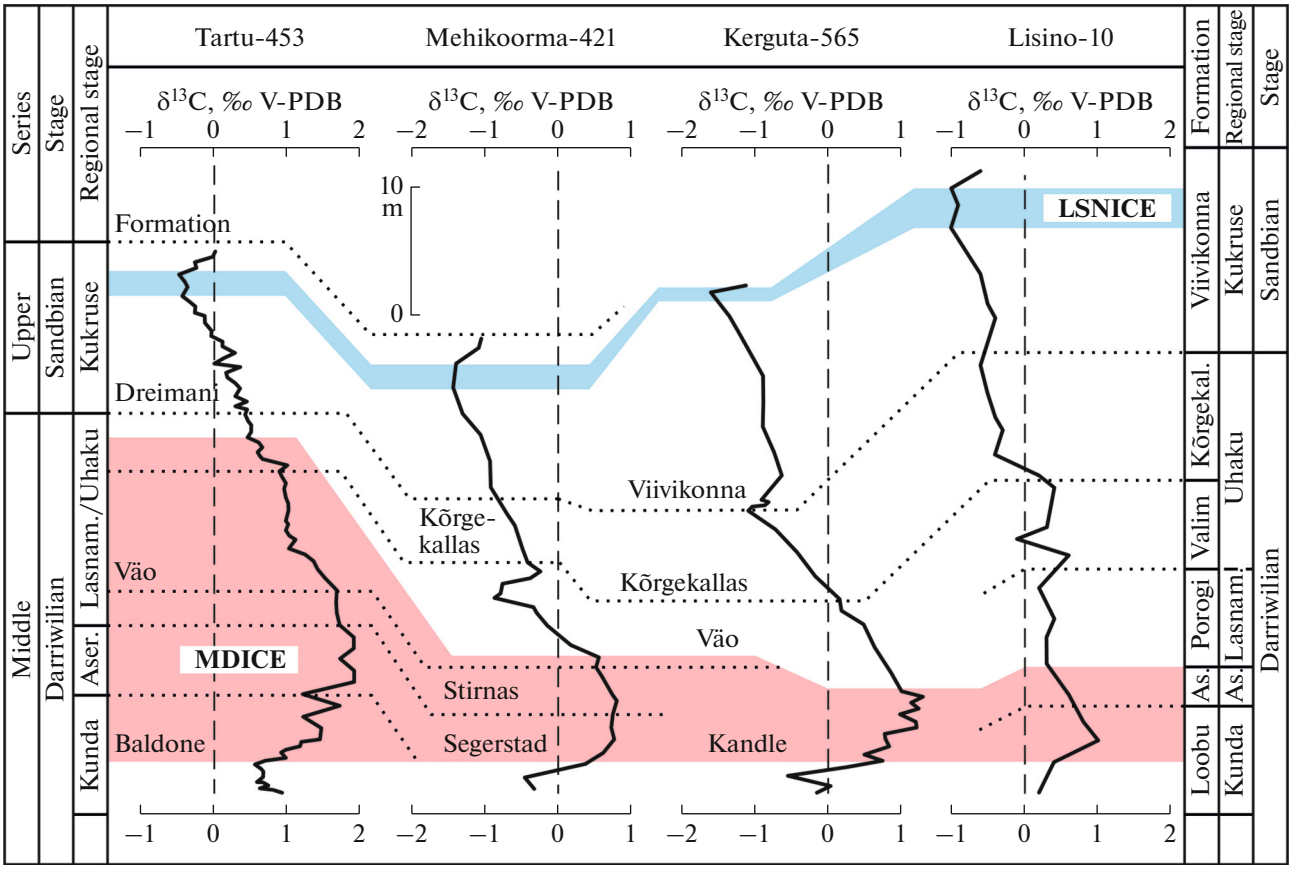


Fig. 8. Correlation of carbon isotope ($\delta^{13}C$) curves across the boundary interval between the Darriwilian and Sandbian stages in the Lisino-10 section with published data from: Tartu-453 borehole (Bauert et al., 2014), Mehikoorma-421 borehole, and Kerguta-565 borehole (Kaljo et al., 2007). Abbreviations: (As., Aser.) Aseri, (Lasnam.) Lasnamägi; (Kõrgekal.) Kõrgekallas.

of substrates favorable for colonization by benthos. Enhanced aeration of water masses and subsequent bioturbation prevented the burial of $\delta^{13}C$-depleted OM in sediments and facilitated its oxidation, which later led to a decrease in $\delta^{13}C$ of pore waters (Zaitsev and Baraboshkin, 2006; Zaitsev and Pokrovsky, 2014). The predominance of oxidizing settings in the northwestern Russian Plate during the Floian–Dapingian time is confirmed by the wide distribution of red-colored deposits and ferruginous goethite–hydrogoethite impregnation of hardground surfaces (Zaitsev and Baraboshkin, 2006). In the sections of the Argentine Precordillera, USA, and Australia, this negative carbon isotope event is also correlated with the regression phase (Buggisch et al., 2003), which allows it to be considered a marker of termination or retardation of carbonate sedimentation in the deeper-water sections, where this carbon-isotopic event is much less pronounced (Munnecke et al., 2011; Wang et al., 2009).

The Middle Darriwilian positive excursion, MDICE (Calner et al., 2014), in the Lisino-10 borehole section is expressed as a low-amplitude (~1‰) positive carbon isotope event spanning the upper half of the Kunda–Aseri regional stages. Peak values of 0.8–1‰ were recorded in the upper part of the Loobu Formation corresponding to the Kunda regional stage of the Northern Baltic region (*Resheniya* ..., 1987). The stratigraphic position of this excursion leaves no doubts and is supported by acritarchs data (Raevskaya and Iskül, 2024). This event is clearly recorded in most sections of the Baltic region and Scandinavia, where it spans an interval from the Kunda to the Uhaku regional stages (Fig. 8) and typically has an amplitude of 1.5–2‰ (Kaljo et al., 2007; Ainsaar et al., 2010). In sections of Baltoscandia, it is frequently expressed as two closely spaced maxima, the lower of which corresponds to the upper part of the Kunda regional stage, while the upper one corresponds to the Aseri regional stage (Bauert et al., 2014; Ainsaar et al., 2020). The Lisino-10 section demonstrates only the lower peak, while the upper peak coincides with a stratigraphic hiatus, which is consistent with strongly reduced thickness of the Aseri interval in the Lisino-10 section.

The mechanism underlying the Middle Darriwilian isotope event remains poorly understood (see overview in (Ainsaar et al., 2020)). It is generally believed that it was caused by the Great Ordovician Biodiversification Event (GOBE), which was

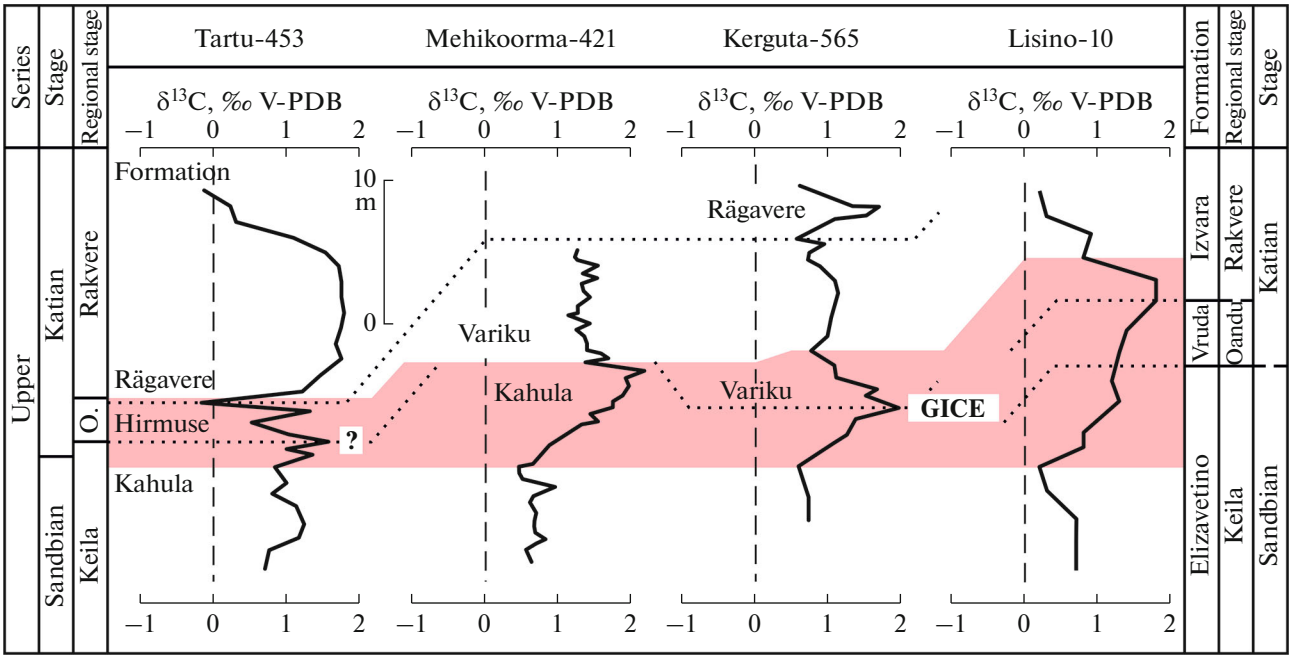


Fig. 9. Correlation of carbon isotope ($\delta^{13}C$) curves across the boundary interval between the Sandbian and Katian stages in the Lisino-10 section with published data from the Männamaa F-367 borehole (Ainsaar and Meidla, 2008), Tartu-453 borehole (Bauert et al., 2014) and Mehikoorma-421 borehole (Kaljo et al., 2007). Abbreviations: (O.) Oandu.

expressed in a sharp increase of biodiversity of marine benthic fauna and the growth of bioproductivity (Schmitz et al., 2008; Zhang et al., 2010; Rasmussen et al., 2016). Ch. Rasmussen et al. (2016) relate the onset of GOBE to a sharp glacioeustatic sea-level drop and a decrease in water temperature, which occurred approximately at the Early–Middle Ordovician boundary.

A negative carbon isotope excursion in the lower Sandbian stage of the Upper Ordovician, LSNICE, has recently been considered as another potential global chemostratigraphic marker (Bauert et al., 2014). In most sections, this excursion is readily recognized by a characteristic inflection in the carbon isotope curve, after which the overall trend shifts toward higher $\delta^{13}C$ values. In the Baltic region, it is confined to the upper part of the Kukruse regional stage and its amplitude rarely exceeds 0.5‰ (Kaljo et al., 2007; Ainsaar et al., 2010; Bauert et al., 2014; Lehnert et al., 2014). A much larger amplitude of the LSNICE (up to 2–2.5‰) was recorded in North American sections (Bergström et al., 2015). In the Lisino-10 section, LSNICE was found in the upper part of the Kukruse regional stage (Viivikonna Formation), where it has an amplitude of about 0.5‰, similar to that in other Baltic sections (Fig. 8).

Small negative carbon isotope events are usually related to the intensification of light carbon-rich river runoff as well as to episodes of tectonomagmatic activity (Saltzman and Thomas, 2012). These factors can produce moderate carbon isotope anomalies, but do not explain the global events. It is suggested that the most significant negative carbon isotope events are typical of sea basins with a weakened connection to the open ocean. In such basins, the appearance of negative carbon isotope anomalies is thought to be related to the sharp episodic incursion of ^{13}C-depleted river waters into the basin, which was controlled by periodic regressions (Panchuk et al., 2005; Saltzman and Edwards, 2017). Another reason for the negative isotope event in the Early Sandbian could be the emergence of terrestrial vegetation at the Early–Middle Ordovician boundary (Steemans et al., 2009; Davies and Gibling, 2010), which resulted in an increase in the rate of soil formation and enhanced the transport of ^{13}C-depleted soil CO_2 into the marine basin. It should be noted that this time coincided with the "Early Caradocian" decline in zoo- and phytoplankton biodiversity in response to eustatic sea-level changes (Dronov and Holmer, 1999; Vecoli and Le Hérissé, 2004; Dronov, 2017). In the Lisino-10 borehole section, this level corresponds to a stratigraphic hiatus, which is recorded in other sections of Baltoscandia (Dronov and Holmer, 1999; Kaljo et al., 2007; Ainsaar et al., 2010; Bauert et al., 2014) and coincides with the boundary of the Tallinn and Kegel sequences (Dronov and Holmer, 1999; Dronov, 2017).

The "Guttenberg" positive carbon excursion, GICE, was initially established in North America (Hatch et al., 1987), from which it later received its name (Saltzman et al., 2003; Ainsaar et al., 2010). It is most distinctly expressed in sections from the USA

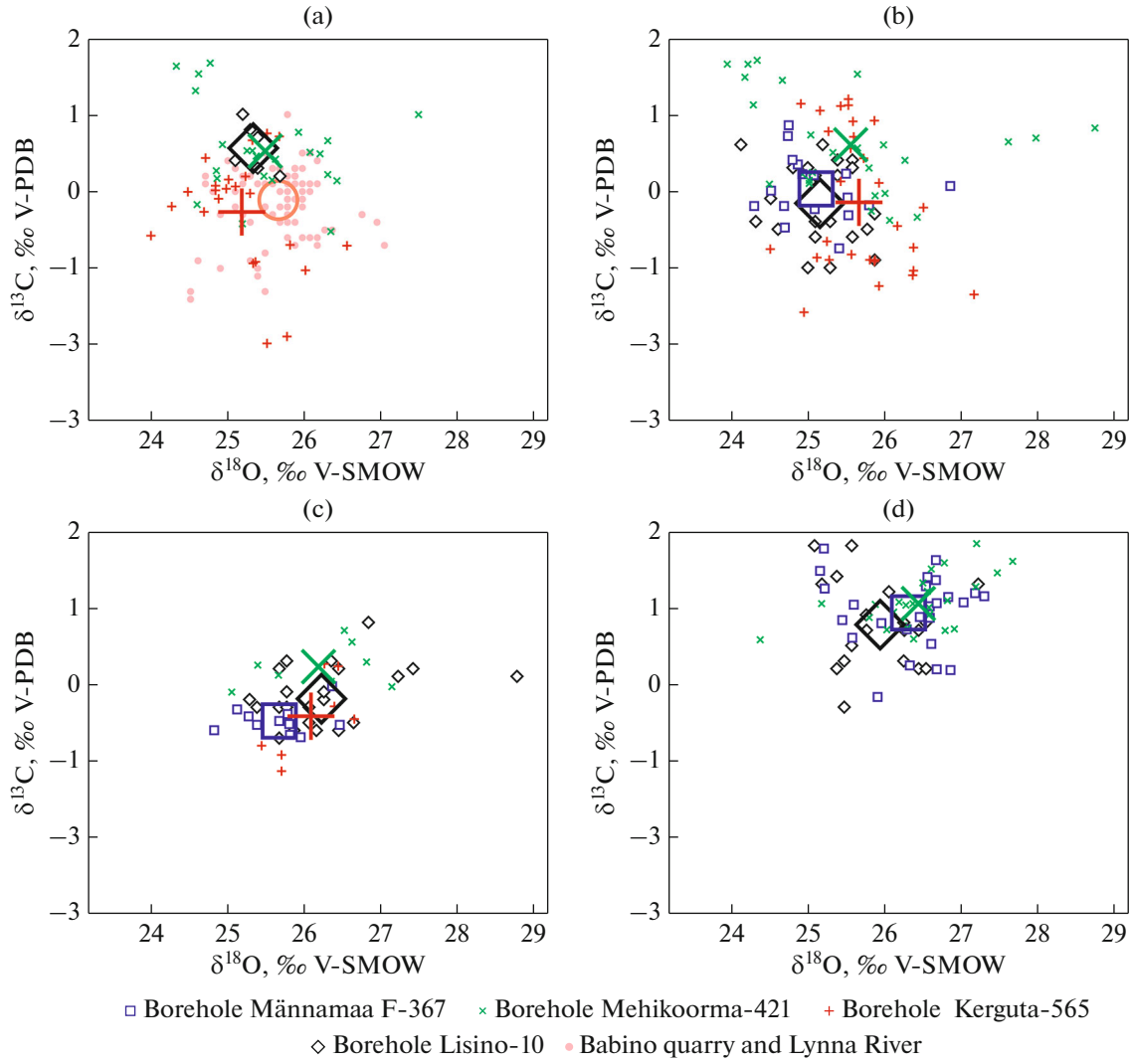


Fig. 10. Carbon and oxygen isotope composition ($\delta^{13}C$ vs. $\delta^{18}O$) of Ordovician carbonate rocks. Data from the Lisino-10 borehole (this study) and other sections in the northern Baltic and Leningrad regions: Männamaa F-367 (Ainsaar and Meidla, 2008), Mehikoorma-421, Kerguta-565 (Kaljo et al., 2007), Babino quarry, and Lynna River (Zaitsev and Pokrovsky, 2014). Values are reported relative to the V-PDB ($\delta^{13}C$) and V-SMOW ($\delta^{18}O$) standards. (a) Volkhov and Kunda regional stages (Dapingian–Lower Darriwilian), (b) Aseri–Kukruse regional stages (Darriwilian–Lower Sandbian), (c) Idavere and Jõhvi regional stages (middle part of the Sandbian Stage), (d) Keila, Oandu and Rakvere regional stages (Upper Sandbian–Lower Katian).

representing different facies types, where its amplitude reaches 4–5‰ and more (Patzkowsky et al., 1997; Saltzman and Young, 2005; Ludvigson et al., 2004; Young et al., 2005; Kaljo et al., 2007). The GICE was also recorded in North and South China (Bergström et al., 2009b; Liu et al., 2016; Zhang et al., 2010), in Sweden (Bergström et al., 2010; Pouille et al., 2013), Norway (Bergström et al., 2011), in Middle and South Baltic regions (Ainsaar and Meidla, 2008; Kaljo et al., 2007; Ainsaar et al., 2010; Bauert et al., 2014; Bauert et al., 2017) and on the Siberian Platform (Pokrovsky et al., 2022). In Baltoscandia, the "Guttenberg" excursion is less pronounced than in the USA. Its amplitude is usually no more than 1–2‰ (Kaljo et al., 2007; Ainsaar et al., 2010; Bergström et al., 2010), reaching 2.5‰ in individual sections of the South Baltic region (Bauert et al., 2017). In the Middle and Northern Estonia, GICE is often partly or completely absent (Fig. 9), and is correlated with large stratigraphic hiatus at the boundary of the Keila and Oandu regional stages (Kaljo et al., 2007; Ainsaar et al., 2010). In many sections of Baltoscandia, the GICE event is associated with a thick bentonite bed (Kinnekulle K-bentonite) containing zircon dated at 454.5 Ma (Kaljo et al., 2007), which corresponds to the Upper Sandbian (Ainsaar et al., 2010). In the Lisino-10 section, GICE spans a significant stratigraphic interval and is expressed as a gradual increase in $\delta^{13}C$ from 0.2‰ in the upper part of the Elizavetino Formation to 1.8‰ in the lower part of the Izvara Formation (Fig. 9). In

North Estonia this interval corresponds to the boundary between the Kahula and Hirmuse formations, and in Central and Southern Estonia, to those of the Kahula and Variku formations, respectively (Kaljo et al., 2007; Ainsaar et al., 2010).

It was noted by different authors that the onset of the "Guttenberg" carbon isotope event with minimum $\delta^{13}C$ values in different-facies sections formed in different paleotectonic and paleogeographic environments is frequently confined to the "clay" intervals, which are enriched (up to 70–80%) in fine silicate material, overlie the regional unconformities, and correspond to the episodes of sharp deepening of the basin. In addition to the enrichment in fine terrigenous material, these levels frequently contain OM-rich interbeds, while their hiatus surfaces are characterized by impregnation with iron phosphates and sulfides (Ludvigson et al., 2004; Young et al., 2005; Bauert et al., 2014). It is generally considered that the GICE formation was determined by a combination of physical, chemical, and biotic factors. Young et al. (2005) proposed a model in which the GICE was caused by periodic upwelling. The global cooling that started at that time could have caused a change in thermohaline circulation of water masses, which facilitated the ascent of cold, deep waters enriched in organic matter, phosphorus, and light carbon isotopes (Baturin, 1999; Patzkowsky et al., 1997). Saturation of bottom waters with nutrients led to increased bioproductivity in the coastal parts of the basin. Periodic faunal die-offs could have created anoxic conditions favorable for iron–phosphate and sulfide mineralization (Ludvigson et al., 2004).

Figure 10 compares the $\delta^{13}C$ and $\delta^{18}O$ isotope compositions from different stratigraphic intervals in the Lisino-10 section and coeval sections of different facies, which were located far away from each other (Kaljo et al., 2007; Ainsaar and Meidla, 2008; Bauert et al., 2014; Zaitsev and Pokrovsky, 2014). For the Lower–Middle Ordovician (Figs. 10a, 10b) and the Upper Ordovician (Figs. 10c, 10d), the average $\delta^{13}C$ and $\delta^{18}O$ values of all presented sections are close, which clearly indicates a "primary" isotope signal discovered in these rocks. The slightly (~1‰) heavier carbon isotope composition in the Volkhov–Kunda interval of the Lisino-10 and Mehikoorma-421 sections is probably related to some facies differences, as well as to the transport and circulation of coastal water masses enriched in meteoric carbon within the basin, which requires further study.

CONCLUSIONS

The Ordovician section of the Lisino-10 borehole at present represents the only section that has provided $\delta^{13}C$ and $\delta^{18}O$ curves for the Floian–lower Katian interval of the northwestern Russian Plate.

The correlation of carbon and oxygen isotope composition in the studied section is absent. This leaves little doubts about the primary (synsedimentary) nature of large carbon isotope events, but suggests that second-order C- and O-isotope variations may be related to diagenesis . Unlike $\delta^{13}C$, the minimum values of which fall in the middle part of the section, the $\delta^{18}O$ values gradually increase upsection at ~3‰, accompanied by a simultaneous increase in dolomite content. Several possible causes can be proposed to explain this trend: (1) enrichment of water in ^{18}O due to evaporation; (2) an increase in oxygen isotope fractionation in the carbonate–water system due to magnesium enrichment of carbonates; (3) the greater resistance of dolomite to post-depositional alteration due to the lower solubility compared to calcite.

Within the Latorp to lower Rakvere interval (Floian to lower Katian stages), two positive carbon isotope events are distinguished in the Lisino-10 borehole: (1) in the middle part of the Darriwilian Stage (MDICE) and (2) at the Sandbian–Katian boundary (GICE). The lower event—the middle Darriwilian positive excursion—is represented only by the lower (Kunda) part and can be confidently correlated with the similar excursion in the Kandle Formation of the Kerguta-565 borehole (North Estonia), as well as in the Segerstad and Stirnas formations of the Mehikoorma-421 borehole (South Estonia, Fig. 8). The upper positive excursion at the boundary of the Keila–Oandu regional stages (GICE) spans an interval of the upper Elizavetino, Vruda, and lower Izvara formations. In the sections of South Estonia (Mehikoorma-421 and Tartu-453 boreholes), this interval is correlated with the boundary deposits of the Kahula and Variku formations (Fig. 9).

In addition to positive $\delta^{13}C$ excursions, the Lisino-10 borehole section demonstrates two negative isotope events: (1) carbon isotope excursion BDNICE in the lower part of the Volkhov Formation (base of the Dapingian Stage); (2) negative carbon isotope event in the lower part of the Sandbian Stage (LSNICE). The Lower Dapingian excursion BDNICE in the Lisino-10 section was recorded in the lowermost sample of the Volkhov Formation. In the northwestern Russian Plate, it corresponds to the large regional erosional unconformity, which makes it difficult to identify in most sections of the northern Baltic region. The LSNICE in the Lisino-10 section is recorded in the upper part of the Viivikonna Formation. On the carbon isotope curve, it is expressed as a characteristic bend and a change from a decreasing to an increasing trend of $\delta^{13}C$. This excursion can be clearly correlated with the similar inflections in the $\delta^{13}C$ curve in the upper part of the Viivikonna Formation of the Kerguta-565 borehole (North Estonia) and from the coeval Dreimani Formation in South Estonia (boreholes Mehikoorma-421 and Tartu-453).

Obtained results allow a reliable chemostratigraphic correlation of the Lisino-10 section with other sections of Baltoscandia and with the global carbon isotope curve. Thus, the Lisino-10 section can be considered a "reference" section for further chemostratigraphic correlation with sections from the Ordovician paleobasin of the Russian Plate and other regions.

ACKNOWLEDGMENTS

The authors are grateful to L.I. Lukyanova, T.Yu. Tolmacheva (A.P. Karpinsky All-Russian Research Geological Institute, VSEGEI), and A.S. Yanovsky (St. Petersburg Complex Geological Expedition) for providing access to the core samples.

FUNDING

The study was carried out in the framework of the state assignment of the Geological Institute of the Russian Academy of Sciences.

CONFLICT OF INTEREST

The authors of this work declare that they have no conflicts of interest.

REFERENCES

Ainsaar, L., Kaljo, D., Martma, T., et al., Middle and Upper Ordovician carbon isotope chemostratigraphy in Baltoscandia: A correlation standard and clues to environmental history, *Palaeogeogr., Palaeoclimat., Palaeoecol.*, 2010, vol. 294, pp. 189–201.
https://doi.org/10.1016/j.palaeo.2010.01.003

Ainsaar, L. and Meidla, T., Ordovician carbon isotopes, Mannamaa (F-367) Drill Core, Poldvere, A., Ed., *Eston. Geol. Sect., Bull.*, 2019, no. 9.

Ainsaar, L., Tinn, O., Dronov, A.V., et al., Stratigraphy and facies differences of the Middle Darriwilian Isotopic Carbon Excursion (MDICE) in Baltoscandia, *Eston. J. Earth Sci.*, 2020, vol. 69, no. 4, pp. 214–222.
https://doi.org/10.3176/earth.2020.16

Albanesi, G.L., Carrera, M.G., Canas, F.L., and Saltzman, M., A proposed global boundary stratotype section and point for the base of the Middle Ordovician Series: The Niquivil section, Precordillera of San Juan, Argentina, *Episodes*, 2006, vol. 29, pp. 1–15.
https://doi.org/10.18814/epiiugs/2006/v29i1/001

Bai, X-L., Zhang, S-N., Huang, Q-Y., Ding, X-Q., and Zhang, S-Y., Origin of dolomite in the Middle Ordovician peritidal platform carbonates in the northern Ordos Basin, western China. *Petrol. Sci.*, 2016, vol. 13, pp. 434–449.
https://doi.org/10.1007/s12182-016-0114-5

Baturin, G.N., Hypotheses of phosphogenesis and the ocean environment, *Lithol. Miner. Resourc.,* 1999, no. 5, pp. 411–430.

Bauert, H., Ainsaar, L., Põldsaar, K., and Sepp, S., The $\delta^{13}C$ chemostratigraphy of the Middle and Upper Ordovician succession in the Tartu-453 drillcore, southern Estonia, and the significance of the HICE, *Eston. J. Earth Sci.*, 2014, vol. 63, no. 4, pp. 195–200.
https://doi.org/10.3176/earth.2014.18

Bauert, H., Hints, O., Bauert, G., et al., The Guttenberg carbon isotope excursion (GICE; Ordovician) in Estonia, in *10th Baltic Stratigr. Conf., Abstracts of Oral and Poster Presentations*, Warszawa: Univ. Warsaw, 2017.

Bergström, S.M., Saltzman, M.R., Leslie, S.A., Ferretti, A., and Young, S.A., Trans-Atlantic application of the Baltic Middle and Upper Ordovician carbon isotope zonation, *Eston. J. Earth Sci.*, 2015, vol. 64, no. 1, pp. 8–12.
https://doi.org/10.3176/earth.2015.02

Bergström, S.M., Schmitz, B., Saltzman, M.R., and Huff, W.D., The Upper Ordovician Guttenberg $\delta^{13}C$ excursion (GICE) in North America and Baltoscandia: Occurrence, chronostratigraphic significance, and paleoenvironmental relationships, Finney, S.C. and Berry, W.B.N., Eds., in *The Ordovician Earth System*, Geol. Soc. Am. Spec. Pap., 2010, pp. 37–67.
https://doi.org/10.1130/2010.2466(04)

Bergström, S.M., Schmitz, B., Young, S.A., and Bruton, D.L., Lower Katian (Upper Ordovician) $\delta^{13}C$ chemostratigraphy, global correlation and sea-level changes in Baltoscandia, *GFF*, 2011, vol. 133, pp. 31–47.
https://doi.org/10.1080/11035897.2011.557162

Bergström, S.M., Xu, C., Gutiérrez-Marco, J.C., and Dronov, A., The new chronostratigraphic classification of the Ordovician System and its relations to major regional series and stages and to $\delta^{13}C$ chemostratigraphy, *Lethaia*, 2009a, vol. 42, no. 1, pp. 97–107.
https://doi.org/10.1111/j.1502-3931.2008.00136.x

Bergström, S.M., Xu, C., Schmitz, B., et al., First documentation of the Ordovician Guttenberg $\delta^{13}C$ excursion (GICE) in Asia: chemostratigraphy of the Pagoda and Yanwashan formations in southeastern China, *Geol. Mag*, 2009b, vol. 146, no. 1, pp. 1–11.
https://doi.org/10.1017/S0016756808005748

Buggisch, W., Keller, M., and Lehnert, O., Carbon isotope record of the Late Cambrian and Early Ordovician carbonates of the Argentine Precordillera, *Palaeogeogr., Palaeoclimatol., Palaeoecol.*, 2003, vol. 195, pp. 357–373.
https://doi.org/10.1016/S0031-0182(03)00365-1

Calner, M., Lehnert, O., Wu, R., Dahlqvist, P., and Joachimski, M.M., $\delta^{13}C$ chemostratigraphy in the Lower–Middle Ordovician succession of Oland (Sweden) and the global significance of the MDICE, *GFF*, 2014, vol. 136, pp. 48–54.
https://doi.org/10.1080/11035897.2014.901409

Davies, N.S. and Gibling, M.R., Paleozoic vegetation and the Siluro-Devonian rise of fluvial lateral accretion sets, *Geology*, 2010, vol. 38, no. 1, pp. pp. 51–54.
https://doi.org/10.1130/G30443.1

Dmitrovskaya, Yu.E., The Moscow Paleobasin in the Early Paleozoic, *Otechestv. Geol.*, 1993, no. 12, pp. 27–34.

Dronov, A.V., Storm sedimentation in the Lower Ordovician carbonate–terrigenous sediments in the civicnity of St. Petersburg, *Byull. MOIP. Ser. Geol.*, 1998, no. 2, pp. 43–51.

Dronov, A.V., *Ordovician sequence stratigraphy of the Siberian and Russian Platforms, Advances in Sequence Stratigraphy. Special Issue. Stratigraphy and Timescale*, Montenari, M., Ed., Elsevier, 2017, vol. 2, pp. 187–241.
https://doi.org/10.1016/bs.sats.2017.07.005

Dronov, A.V. and Holmer, L.E., Depositional sequences in the Ordovician of Baltoscandia, in *Quo vadis ordovician? Short Papers, 8th Int. Symp. Ordovician System*, Praha: Geol. Acta Univ.Carolinae, 1999.

Dronov, A. and Rozhnov, S., *Climatic changes in the Baltoscandian basin during the Ordovician: sedimentological and palaeontological aspects*, *Acta Palaeont. Sinica*, 2007, vol. 46.

Dronov, A.V., Tolmacheva, T.Yu., and Iskyul, G.S., Ordovician of the, St. Petersburg Region, in *13th Int. Symp. Ordovician System (Guidebook of the Pre-Symposium Field Trip*, St. Petersburg: VSEGEI, 2019.

Dronov, A.V., Koren, T.N., Popov, L.E., and Tolmacheva, T.Yu., *Metodika sobytiinoi stratigrafii v obosnovanii korrelyatsii regional'nykh stratonov na primere nizhnego ordovika Severo-Zapada Rossii* (Methodology of event stratigraphy in the correlation of regional stratigraphic units: an example from the Lower Ordovician of Northwest Russia), St. Petersburg: VSEGEI, 1998.

Edwards, C.T. and Saltzman, M.R., Carbon isotope ($\delta^{13}C_{carb}$) stratigraphy of the Lower–Middle Ordovician (Tremadocian–Darriwilian) in the Great Basin, western United States: Implications for global correlation, *Palaeogeogr., Palaeoclimatol., Palaeoecol.*, 2014. V. 399. P. 1–20. https://doi.org/10.1016/j.palaeo.2014.02.005

Fortunatova, N.K., Kartseva, O.A., Baranova, A.V., Agafonova, G.V., and Ofman, I.P., *Atlas strukturnykh komponentov karbonatnykh porod* (Atlas of Structural Components in Carbonate Rocks), Moscow: VNIGNI, 2005.

Friedman, I. and O'Neil, J.R., *Compilation of stable isotope fractionation factors of geochemical interest. Data of Geochemistry*, Geol. Surv. Prof. Pap., no. 440.

Gregg, J.M. and Sibley, D.F., Epigenetic dolomitization and the origin of xenotopic dolomite texture, *J. Sediment. Petrol.*, 1984, vol. 54, no. 3, pp. 908–931.

Hatch, J.R., Jacobson, S.R., Witzke, B.J., et al., Possible Late-Middle Ordovician carbon isotope excursion: evidence from Ordovician oils and hydrocarbon source rocks, mid-continent and east-central United States, *Am. Ass. Petrol. Geol. Bull.*, 1987, vol. 71, pp. 1342–1354. https://doi.org/10.1306/703C8074-1707-11D7-864500010-2C1865D

Huang, B., Zhang, S., Lu, Z., et al., Origin of dolomites in Lower-Middle Ordovician carbonate rocks in the Yingshan Formation, Gucheng Area, Tarim Basin: Evidence from petrography and geochemical data, *Mar. Petrol. Geol.*, 2021, vol. 134, p. 105322. https://doi.org/10.1016/j.marpetgeo.2021.105322

Ivantsov, A.Yu. and Mel`nikova, L.M., The Azeri, Lasnamagi, and Uhaku Ordovician horizons of the Leningrad region and their trilobites and ostracode faunas, *Stratigr. Geol. Correl.*, 2003, vol. 11, no. 4, pp. 332—347.

Jaanusson, V., Aspects of carbonate sedimentation in the Ordovician of Baltoscandia. *Lethnia*, 1972, vol. 6, pp. 11–34.

Jaanusson, V., Confacies differentiation and Upper Middle Ordovician correlation in the Baltoscandian Basin. *Proc. Estonian. Acad. Sci. Geol.*, 1995, vol. 44, no. 2, pp. 73–86.

Kaljo, D., Martma, T., and Saadre, T., Post-Hunnebergian Ordovician carbon isotope trend in Baltoscandia, its environmental implications and some similarities with that of Nevada, *Palaeogeogr., Palaeoclimatol., Palaeoecol.*, 2007, vol. 245, pp. 138–155. https://doi.org/10.1016/j.palaeo.2006.02.020

Kump, L.R., The geochemistry of mass extinction, *Treatise on Geochemistry*, 2003, vol. 7, pp. 13–19. https://doi.org/10.1016/B0-08-043751-6/07101-2

Lehnert, O., Meinhold, G., Wu, R., Calner, M., and Joachimski, M.M., The $\delta^{13}C$ chemostratigraphy in the upper Tremadocian through lower Katian (Ordovician) carbonate succession of the Siljan district, central Sweden, *Eston. J. Earth Sci.,* 2014, vol. 63, no. 4, pp. 277–286. https://doi.org/10.3176/earth.2014.31

Liang, J., Azmy, K., Li, K., et al., Petrographic and geochemical characteristics of the Middle Upper Cambrian Xixiangchi dolomites in the central Sichuan Basin, southwest China: Implications for dolomite origins and dolomitization mechanisms, *Mar. Petrol.Geol.,* 2023, vol. 152, p. 106215. https://doi.org/10.1016/j.marpetgeo.2023.106215

Liu, C.-G., Qi, L.-X., and Liu, Y.-L., Positive carbon isotope excursions: global correlation and genesis in the Middle-Upper Ordovician in the northern Tarim Basin, Northwest China, *Petrol. Sci.*, 2016, vol. 13, pp. 192–203. https://doi.org/10.1007/s12182-016-0096-3

Korobov, A.D., Ahlestina, E.F., Korobova, L.A., et al., Authigenic dolomite in the organic-rich rocks of the Bazhenov Formation—the evidence for active syngenetic naphthide genesis, *Izv. Saratov. Univ., Ser. Earth Sci.*, 2018, vol. 18, no. 1, pp, 50–53. https://doi.org/10.18500/1819-7663-2018-18-1-50-53

Kotlukov, V.A. and Mitgarts, B.B., *Strukturno-tektonicheskie osobennosti severnoi chasti Pribaltiki v predelakh lista O-35* (Structural and Tectonic Features of the Northern Baltic Region, Sheet 0-35), Moscow: Gosgeoltekhizdat, 1955.

Leeder, M.R., *Sedimentology. Process and Product*, London: Allen Unwin, 1982.

Ludvigson, G.A., Witzke, B.J., Gonzalez, L.A., et al., Late Ordovician (Turinian–Chatfieldian) carbon isotope excursions and their stratigraphic and paleoceanographic significance, *Palaeogeogr., Palaeoclimatol., Palaeoecol.*, 2004, vol. 210, pp. 187–214.

Lyutkevich, E.M., Ievian stage of the Silurian plateau in the Baltic region, *Byull. MOIP, Otd. Geol.*, 1939, vol. 17, nos. 4–5, pp. 135–141.

Maslov, V.P., Fossil calcareous algae in the USSR, *Tr. GIN AN USSR*, 1956, no. 160.

Maslov, V.P., Algae and carbonate precipitation, *Izv. AN SSSR, Ser. Geol.*, 1961, no. 12, p. 81–86.

Melezhik, V.A., Roberts, D., Fallick, A.E., Gorokhov, I.M., and Kusnetzov, A.B., Geochemical preservation potential of high-grade calcite marble versus dolomite marble: implication for isotope chemostratigraphy. *Chem. Geol.*, 2005, vol. 216, pp. 203–224. https://doi.org/10.1016/j.chemgeo.2004.11.020

Munnecke, A., Zhang, Y., Liu, X., and Cheng, J., Stable carbon isotope stratigraphy in the Ordovician of South China, *Palaeogeogr., Palaeoclimatol., Palaeoecol.*, 2011, vol. 307, pp. 17–43. https://doi.org/10.1016/j.palaeo.2011.04.015

Myannil, R.M., *Istoriya razvitiya Baltiiskogo basseina v ordovike* (History of the Baltic Basin evolution in the Ordovician), Tallin: Valgus, 1966.

Nizhnii paleozoi okrestnostei Sankt-Peterburga (Lower Paleozoic in the St. Petersburg Region), compiled by Dronov, A.V., Tolmacheva, T.Yu, and Iskul, G.S., St. Petersburg, 2012.

Panchuk, K.M., Holmden, C., and Kump, L.R., Sensitivity of the epeiric sea carbon isotope record to local-scale carbon cycle processes: tales from the Mohawkian sea, *Palaeogeogr., Palaeoclimatol., Palaeoecol.*, 2005, vol. 228, pp. 320–337.
https://doi.org/10.1016/j.palaeo.2005.06.019

Patzkowsky, M.E., Slupik, L.M., Arthur, M.A., Pancost, R.D., and Freeman, K.H., Late Middle Ordovician environmental change and extinction: Harbinger of the Late Ordovician or continuation of Cambrian patterns?, *Geology*, 1997, vol. 25, no. 10, pp. 911–914.

Pokrovsky, B.G., Zaitsev, A.V., Dronov, A.V., et al., C, O, S, and Sr isotope geochemistry and chemostratigraphy of Ordovician sediments in the Moyero River section, northern Siberian Platform, *Lithol. Miner. Resourc.*, 2018, no. 4, pp. 283–306.
https://doi.org/10.7868/S0024497X18040031

Pokrovsky, B.G., Bujakaite, M.I., Kolesnikova, A.A., Petrov, O.L., and Khlebnikov, M.S., C, O, and Sr isotope geochemistry of the Vendian Shuram–Wonoka anomaly and associated metasedimentary rocks in the inner part of the Patom Upland (Central Siberia), *Lithol. Miner. Resourc.*, 2021, no. 5, pp. 390–417.
https://doi.org/10.31857/S0024497X21050049

Pokrovsky, B.G., Zaitsev, A.V., Bujakaite, M.I., and Dronov, A.V., The C–O–Sr–S isotope geochemistry and chemostratigraphic correlation of Ordovician deposits in the Vilyui structural-facies zone, Siberian Platform, *Lithol. Miner. Resourc.*, 2022, no. 6, pp. 518–542.
https://doi.org/10.31857/S0024497X22060052

Pouille, L., Delabroye, A., Vandenbroucke, T.R.A., et al., Chitinozoan biostratigraphy across the Katian (Late Ordovician) GICE event in the Borenshult-1 drillcore (Sweden), *Rev Palaeobot. Palynol.,* 2013, vol. 198. p. 134–144.
https://doi.org/10.1016/j.revpalbo.2013.05.007

Pylma, L., *Sravnitel'naya litologiya karbonatnykh porod ordovika severnoi i srednei Pribaltiki* (Comparative Lithology of Ordovician Carbonate Rocks in the Northern and Central Baltic Region), Inst. Geol. AN Eston. SSR, Tallin: Valgus, 1982.

Raevskaya, E.G. and Iskül, G.S. Middle-Upper Ordovician acritarchs from Baltoscandia (Lisino- 10 borehole, Leningrad region) and their biostratigraphic implication, *Paleontol. J.*, 2024, vol. 58, no. 9, pp. 1075–1088.
https://doi.org/10.1134/S0031030124600835

Raevskaya, E. and Zaitsev, A., Acritarch based biostratigraphy of the Ordovician, in *Moscow: syneclise, East-European Platform*, 4th Ann.Meet. IGCP 591, Estonia, Abstracts and Field Guide, 2014.

Rasmussen, C.M.Ø., Ullmann, C.V., Jakobsen, K.G., et al., Onset of main Phanerozoic marine radiation sparked by emerging Mid Ordovician icehouse, *Sci. Rep.*, 2016, no. 6 (18884),
https://doi.org/10.1038/srep18884

Resheniya mezhvedomstvennogo stratigraficheskogo soveshchaniya po ordoviku i siluru Vostochno-Evropeiskoi platformy Resheniya mezhvedomstvennogo stratigraficheskogo soveshchaniya po ordoviku i siluru Vostochno-Evropeiskoi platformy, 1984 (Resolutions of the Interdepartmental Stratigraphic Committee on the Ordovician and Silurian in the East European Platform, 1984), Leningrad: VSEGEI, 1987.

Saltzman, M.R. and Edwards, C.T., Gradients in the carbon isotopic composition of Ordovician shallow water carbonates: A potential pitfall in estimates of ancient CO_2 and O_2, *Earth Planet. Sci. Lett.*, 2017, vol. 464, pp. 46–54.
https://doi.org/10.1016/J.EPSL.2017.02.011

Saltzman, M.R. and Thomas, E., Carbon isotope stratigraphy, in *The Geologic Time Scale*, Gradstein, F.M., Ogg, J.G., Schmitz, M.D., and Ogg, G.M., Eds., Boston: Elsevier, 2012, pp. 207–233.
https://doi.org/10.1016/B978-0-444-59425-9.00011-1

Saltzman, M.R. and Young, S.A., Long-lived glaciation in the Late Ordovician? Isotopic and sequence-stratigraphic evidence from western Laurentia, *Geology*, 2005, vol. 33, no. 2, pp. 109–112.
https://doi.org/10.1130/G21219.1

Saltzman, M.R., Bergström, S.M., Huff, W.D., and Kolata, D.R., Conodont and graptolite biostratigraphy and Ordovician (Early Chatfieldian, Middle Ordovician) $\delta^{13}C$ excursion in North America and Baltoscandia: implications for the interpretation of the relations between the Millbrig and Kinnekulle k-bentonites, *Ordovician from the Andes: INSUGEO, Serie Correlacion Geologica,* Albanesi, G.L., Beresi, M.S., and Peralta, S.H., Eds., Tucuman: Univ. Nacion. Tucuman, 2003, vol. 17, pp. 137–142.

Schmitz, B., Harper, D.A.T., Peucker-Ehrenbrink, B., et al., Asteroid breakup linked to the Great Ordovician Biodiversification Event, *Nature Geosci.*, 2008, vol. 1, pp. 49–53.
https://doi.org/10.1038/ngeo.2007.37

Selivanova, V.A., The Ordovician System, in *Geologiya SSSR* (Geology of the Soviet Union), Moscow: Nedra, 1971, vol. 1 (Leningrad, Pskov, and Novgorod regions), pp. 127–173.

Steemans, P., Le Hérissé A., Melvin J., et al., Origin and radiation of the earliest vascular land plants, *Science*, 2009, vol. 324, p. 353.
https://doi.org/10.1126/science.1169659

Vecoli, M. and Le Hérissé A. Biostratigraphy, taxonomic diversity and patterns of morphological evolution of Ordovician acritarchs (organicwalled microphytoplankton) from the northern Gondwana margin in relation to palaeoclimatic and palaeogeographic changes, *Earth Sci. Rev.*, 2004, vol. 67, pp. 267–311.
https://doi.org/10.1016/j.earscirev.2004.03.002

Veizer, J., Ala, D., Azmy, K., et al., $^{87}Sr/^{86}Sr$, $\delta^{13}C$ and $\delta^{18}O$ evolution of Phanerozoic seawater, *Chem. Geol.*, 1999, vol. 161, pp. 59–88.
https://doi.org/10.1016/S0009-2541(99)00081-9

Verbitsky, V.R., Verbitsky, I.V., Vasilieva, O.V., et al., *Gosudarstvennaya geologicheskaya karta Rossiiskoi Federatsii. Masshtab 1 : 1000000. Seriya Tsentral'no-Evropeiskaya* (State Geological Map of the Russian Federation. Scale 1 : 1000000, Ser. Central Europe. Sheet 0-35-Pskov, Explanatory Note), St. Petersburg: Kartogr. Fabr. VSEGEI, 2012.

Wang, X., Stouge, S., Xu, C., et al., The global stratotype section and point for the base of the Middle Ordovician Series and the Third Stage (Dapingian), *Episodes*, 2009, vol. 32, no. 2, pp. 96–113.
https://doi.org/10.18814/epiiugs/2009/v32i2/003

Young, S.A., Saltzman, M.R., and Bergström, S.M., Upper Ordovician (Mohawkian) carbon isotope ($\delta^{13}C$) stratigraphy in eastern and central north america: regional expression of a perturbation of the global carbon cycle, *Palaeogeogr., Palaeoclimatol., Palaeoecol.*, 2005, vol. 222, pp. 53–76.
https://doi.org/10.1016/j.palaeo.2005.03.008

Zaitsev, A.V. and Baraboshkin, E.Yu., Stratigraphic hiatuses in the Billingenian-Kundan deposits (Lower–Middle Ordovician) in the central and eastern parts of the Baltic–Ladoga Klint, *Mosc. Univ. Geol. Bull.*, 2006, no. 3, pp. 157–175.

Zaitsev, A.V. and Pokrovsky, B.G., Carbon and oxygen isotope compositions of Lower–Middle Ordovician carbonate rocks in the northwestern Russian Platform, *Lithol. Miner. Resourc.*, 2014, vol. 49, no. 3, 272–289.
https://doi.org/10.1134/S0024490214030079

Zhang, T., Shen, Y., and Algeo, T.J., High-resolution carbon isotopic records from the Ordovician of South China: Links to climatic cooling and the Great Ordovician Biodiversification Event (GOBE), *Palaeogeogr., Palaeoclimatol., Palaeoecol.*, 2010, vol. 289, pp. 102–112.
https://doi.org/10.1016/j.palaeo.2010.02.020

Zhemchugova, V.A. and Maslova, E.E., Secondary dolomitization as a factor controlling reservoir properties of the Lower Devonian rocks on the eastern flank of the Khoreiver depression (Timan–Pechora oil-and-gas-bearing basin), *Mosc. Univ. Geol. Bull.*, 2020, no. 3, pp. 353–362.
https://doi.org/10.33623/0579-9406-2020-3-47-56

Translated by M. Bogina

Publisher's Note. Pleiades Publishing remains neutral with regard to jurisdictional claims in published maps and institutional affiliations.
AI tools may have been used in the translation or editing of this article.